Molecular Pharmacology Fast Forward. Published on September 4, 2013 as doi: 10.1124/mol.113.086843
This article has not been copyedited and formatted. The final version may differ from this version.

MOL #86843

Title Page

Flavanones that selectively inhibit TRPM3 attenuate thermal nociception *in vivo*

Isabelle Straub, Ute Krügel, Florian Mohr, Jens Teichert, Oleksandr Rizun, Maik Konrad, Johannes Oberwinkler and Michael Schaefer

Rudolf-Boehm-Institut für Pharmakologie und Toxikologie, Universität Leipzig, Leipzig, Germany

Affiliations: Rudolf-Boehm-Institut für Pharmakologie und Toxikologie, Universität Leipzig, Leipzig, Germany (I.S., U.K., M.S., J.T.); Institut für Physiologie und Pathophysiologie, Philipps-Universität Marburg, Marburg, Germany (F.M., O.R., M.K., J.O.)

Molecular Pharmacology Fast Forward. Published on September 4, 2013 as DOI: 10.1124/mol.113.086843
This article has not been copyedited and formatted. The final version may differ from this version.

Running Title Page

Running title: **Selective TRPM3 inhibitors**

Corresponding author: Michael Schaefer, Rudolf-Boehm-Institut für Pharmakologie und Toxikologie, Härtelstr. 16-18, 04107 Leipzig, Germany, phone: +49 341 9724600, fax: +49 341 9724609, e-mail: michael.schaefer@medizin.uni-leipzig.de

Bibliography:

- Number of text pages: 26
- Number of tables: 0
- Number of figures: 12
- Number of references: 37

Word count:

- Abstract: 240
- Introduction: 391
- Discussion 1636

Abbreviations:

$[Ca^{2+}]_i$, intracellular free Ca^{2+} concentration; DRG, dorsal root ganglion; HBS, HEPES-buffered solution; HEK, human embryonic kidney; PregS, pregnenolone sulphate; TRPA, transient receptor potential ankyrin-like; TRPM, transient receptor potential melastatin-related; TRPV, transient receptor potential vanilloid-related

Molecular Pharmacology Fast Forward. Published on September 4, 2013 as DOI: 10.1124/mol.113.086843
This article has not been copyedited and formatted. The final version may differ from this version.

Abstract

TRPM3 (melastatin-related transient receptor potential 3) is a calcium-permeable nonselective cation channel that is expressed in a subset of dorsal root (DRG) and trigeminal ganglia sensory neurons. TRPM3 can be activated by the neurosteroid pregnenolone sulphate (PregS) and heat. $TRPM3^{-/-}$ mice display an impaired sensation of noxious heat and thermal hyperalgesia. We have previously shown that TRPM3 is blocked by the citrus fruit flavanones hesperetin, naringenin and eriodictyol as well as by ononetin, a deoxybenzoin from *Ononis spinosa*. To further improve the tolerability, potency and selectivity of TRPM3 blockers, we conducted a hit optimization procedure by re-screening a focused library that was composed of chemically related compounds. Within newly identified TRPM3 blockers, isosakuranetin and liquiritigenin displayed favorable properties with respect to their inhibitory potency and a selective mode of action. Isosakuranetin, a flavanone whose glycoside is contained in blood oranges and grapefruits, displayed an IC_{50} of 50 nM, and is to our knowledge the most potent inhibitor of TRPM3 identified so far. Both compounds exhibited a marked specificity for TRPM3 compared with other sensory TRP channels, and blocked PregS-induced $[Ca^{2+}]_i$ signals and ionic currents in freshly isolated DRG neurons. Furthermore, isosakuranetin and previously identified hesperetin significantly reduced the sensitivity of mice to noxious heat and PregS-induced chemical pain. Since the physiological functions of TRPM3 channels are still poorly defined, the development and validation of potent and selective blockers is expected to contribute to clarifying the role of TRPM3 *in vivo*.

Molecular Pharmacology Fast Forward. Published on September 4, 2013 as DOI: 10.1124/mol.113.086843
This article has not been copyedited and formatted. The final version may differ from this version.

Introduction

Transient receptor potential melastatin 3 (TRPM3) is a member of the large superfamily of TRP ion channels. The TRPM3 gene encodes a number of different alternative splice variants (Lee, et al., 2003;Oberwinkler, et al., 2005;Frühwald, et al., 2012). Alternative splicing within exon 24 affects the putative pore region, resulting in distinct biophysical properties of the permeation pathway. The TRPM3α1 variant is predominantly selective for monovalent cations whereas TRPM3α2, a 12 amino acid shorter variant, forms a calcium-permeable poorly selective cation channel (Oberwinkler, et al., 2005).

TRPM3α2 channels can be activated by the neurosteroid pregnenolone sulphate (PregS), nifedipine (Wagner, et al., 2008), D-erythro-sphingosine (Grimm, et al., 2005), and by noxious heat (Vriens, et al., 2011). TRPM3 is functionally expressed in insulin-secreting pancreatic beta cells and its activation has been linked to insulin secretion (Wagner, et al., 2008). Furthermore, TRPM3α2 is expressed in neurons of dorsal root ganglia (DRG) and trigeminal ganglia, where it contributes to the detection of noxious heat in healthy and inflamed tissue (Vriens, et al., 2011). Activation of TRPM3 has also been coupled to vascular smooth muscle cell contraction (Naylor, et al., 2010), to oligodendrocyte differentiation, and to neuronal myelination (Hoffmann, et al., 2010).

Recently, we showed that TRPM3 is blocked by citrus fruit flavanones and fabacea secondary metabolites (Straub, et al., 2013). Flavanones, a subgroup of flavonoids, comprise the most common group of plant-derived polyphenolic compounds in the human diet (Manach, et al., 2004). Flavonoids share a common structure: they consist of two aromatic rings (A and B rings) that are linked with a heterocycle (C ring) (Fig. 1A). They can be divided into different subgroups, depending on the oxidation of the C ring, the hydroxylation pattern of the phenolic rings, and the substitution at the 3-position.

Molecular Pharmacology Fast Forward. Published on September 4, 2013 as DOI: 10.1124/mol.113.086843
This article has not been copyedited and formatted. The final version may differ from this version.

For a better understanding of the biologically active flavonoid substructure that bears responsibility for TRPM3-block, we performed a rescreening of a focused library that was composed of members of different flavonoid subgroups and of flavanones with different substitutions on specified positions. Within the flavonoids, only substances that comprise a flavanone backbone displayed a biological activity to block TRPM3. Within the flavanones, we identified isosakuranetin and liquiritigenin as novel potent and specific TRPM3 blockers. The novel identified compounds blocked endogenously expressed TRPM3 in freshly isolated DRG neurons. Furthermore, we demonstrate that isosakuranetin and the previously identified hesperetin block TRPM3-related nociception *in vivo*.

Molecular Pharmacology Fast Forward. Published on September 4, 2013 as DOI: 10.1124/mol.113.086843
This article has not been copyedited and formatted. The final version may differ from this version.

Materials and Methods

Cell culture

HEK293 cells used for transient transfection were cultured in Earle's Minimum Essential Medium (MEM) (Invitrogen), supplemented with 10% fetal calf serum, 2 mM L-glutamine, 100 units ml^{-1} penicillin, and 0.1 mg ml^{-1} streptomycin. HEK293 cells stably expressing myc-tagged mouse TRPM3α2 (HEK_{mTRPM3}) were obtained and maintained as described elsewhere (Frühwald, et al., 2012;Straub, et al., 2013). HEK293 cells stably expressing other sensory TRP channels (HEK_{hTRPA1}, $HEK_{hTRPM8:CFP}$, $HEK_{rTRPV1:YFP}$) were obtained by a limiting dilution method as described recently (Hellwig, et al., 2004;Urban, et al., 2012). Stably transfected cell lines were selected and maintained in HEK293 medium (see above), containing 400 µg ml^{-1} G418. All cells were grown at 37 °C in a humidified atmosphere containing 5% CO_2. Unless otherwise stated, cells were seeded 24 h prior to the experiments onto poly-L-lysine-coated coverslips.

Cell transfection

HEK293 cells were transiently transfected with a bi-cistronic expression plasmid, encoding Myc-tagged TRPM1 and enhanced green fluorescent protein (GFP) as previously described (Lambert, et al., 2011;Straub, et al., 2013). For heat activation of TRPM3, HEK293 cells were transiently transfected with a bi-cistronic plasmid encoding TRPM3α2 and a GFP protein. For detailed information see (Straub, et al., 2013)s.

DRG neuron preparation

8 week-old male and female Wistar rats were sacrificed by an overdose of CO_2. To expose the spinal cord, a careful single dorsal-midline incision along the entire length of the body was made. The spinal cord was then gently removed and dorsal root ganglia from all cervical, thoracic and lumbar segments were obtained. Ganglia were digested for 35 minutes at 37°C in an enzyme solution, containing 1.5 mg ml^{-1} collagenase (Sigma) and 3 mg ml^{-1} dispase (Roche), in HBSS

Molecular Pharmacology Fast Forward. Published on September 4, 2013 as DOI: 10.1124/mol.113.086843
This article has not been copyedited and formatted. The final version may differ from this version.

(Gibco). After repeated trituration with a 1-ml pipette and termination of the digestion by adding 100 µl FCS, the cell suspension was centrifuged (3.5 minutes at 670 g) and resuspended in DMEM medium, supplemented with 5% FCS, 100 units ml^{-1} penicillin, and 0.1 mg ml^{-1} streptomycin. DRG neurons used for measurement of TRPA1-related Ca^{2+} entry were resuspended in a DMEM medium additionally supplemented with 100 ng ml^{-1} nerve growth factor (NGF). Subsequently, droplets of cell suspension were plated on poly-L-lysine (1 mg ml^{-1}, Sigma)-coated coverslips, placed in a culture dish and left to adhere for at least 1 hour in an incubator (37 °C, 5% CO_2). Afterwards, the culture dish was then filled with DMEM medium. All experiments were performed within 36 hours after preparation.

Intracellular Ca^{2+} analysis in cell suspensions

All fluorometric assays in cell suspensions were performed in 384-well plates. For detailed information see (Nörenberg, et al., 2011;Straub, et al., 2013). Shortly, HEK293 cells stably expressing TRPM3 were incubated with fluorescence-indictor dye Fluo-4/AM (4 µM; Molecular Probes Invitrogen) for 30 min at 37 °C, washed and resuspended in HBS buffer, containing 135 mM NaCl, 6 mM KCl, 1 mM $CaCl_2$, 1 mM $MgCl_2$, 5.5 mM D-glucose, and 10 mM HEPES adjusted to pH 7.4 with NaOH. Fluorescence was monitored with a filter-based plate reader device (Polastar Omega, BMG Labtech, Offenburg, Germany) in the bottom-read mode, applying 485\10-nm and 520\20-nm band pass filters for excitation and emission, respectively. Measurements of agonistic properties of the compounds were performed using a custom-made fluorescence plate imaging device built into a robotic liquid handling station (Freedom Evo 150, Tecan, Switzerland), as recently described (Noerenberg, et al., 2012).

Single cell calcium measurement

Molecular Pharmacology Fast Forward. Published on September 4, 2013 as DOI: 10.1124/mol.113.086843
This article has not been copyedited and formatted. The final version may differ from this version.

Single cell measurement of $[Ca^{2+}]_i$ in rat DRG neurons and in transiently transfected HEK293 cells were performed as previously described (Straub, et al., 2013). All measurements were performed at room temperature (22-24 °C).

Whole cell patch clamp measurements

All electrophysiological measurements were performed in the whole-cell voltage-clamp mode at room temperature, using an Axopatch 200B amplifier, connected to a desktop computer via a Digidata 1200 digitizer (Axon CNS, Molecular Devices, Sunnyvale, CA, USA) under the control of the Pclamp 9 or Pclamp10 software (Molecular Devices). To obtain I/V curves, V_h was set to -113 mV for 100 ms, and voltage ramps from -113 to + 87 mV (0.4 mV ms^{-1}) were applied once per second. The inter-sweep holding potential was -13 mV. Concentration response curves were obtained with a voltage step protocol, by repeatedly applying a V_{clamp} of -113 mV and +87 mV (duration of 50 ms, each) every 200 ms. TRPM3 currents typically reached a steady state within less than 15 ms and were averaged over a time window of 20-50 ms after applying voltage steps. The intracellular solution contained 80 mM Cs-aspartate, 45 mM CsCl, 4 mM Na_2ATP, 10 mM HEPES, 10 mM BAPTA, 5 mM EGTA pH 7.2 adjusted with CsOH. The osmolarity was 300–315 mosm. The extracellular solution used contained 145 mM NaCl, 3 mM KCl, 10 mM CsCl, 2 mM $CaCl_2$, 2 mM $MgCl_2$, 10 mM HEPES, 10 mM D-glucose, pH 7.4 adjusted with NaOH. The Cs^+-based, divalent-free external solution for TRPM7 measurements contained 130 mM CsCl, 50 mM mannitol, 10 mM HEPES, pH 7.4 with CsOH. The liquid junction potential between the bath and the pipette solutions was 13 mV (calculated with Clampex, Axon Instr.) and corrected. Series resistances were <10 MΩ and were compensated by 75-85%. The sampling rate was 5 kHz in standard whole cell measurements. For whole-cell measurements in DRG neurons, the extracellular solution contained 140 mM NaCl, 4 mM KCl, 2 mM $MgCl_2$, 100 nM tetrodotoxin, 10 mM TRIS (pH 7.4 with HCl), and the pipette solution contained 140 mM CsCl, 0.6 mM $MgCl_2$, 1 mM EGTA, 10 mM HEPES, 5 mM TEA (pH 7.2 with CsOH). To determine the I-V relationship of

Molecular Pharmacology Fast Forward. Published on September 4, 2013 as DOI: 10.1124/mol.113.086843
This article has not been copyedited and formatted. The final version may differ from this version.

PregS-induced currents, measurements were performed under monovalent free extracellular conditions to suppress other cationic conductance present in DRG neurons. The monovalent free solution contained 2 mM $CaCl_2$, 2 mM $MgCl_2$, 10 mM HEPES, 280 mM D-Mannitol (pH 7.4 with NMDG). The holding potential for measurements in DRG neurons was -60 mV between voltage ramps. Voltage ramps were applied as described for measurements in HEK293 cells. Modulators were applied via a SF-77B Perfusion Fast Step system (Warner Instruments). Heat activation of TRPM3 was performed as described earlier (Straub, et al., 2013). Shortly, solutions were heated with an inline solution heater (Warner Instruments) under control of a TC-324B heater (Warner Instruments). The temperature of the solutions was recorded with the pClamp 10 software.

Giant excised patch electrophysiology

Experiments were performed with oocytes from *Xenopus laevis* obtained from EcoCyte Bioscience. A cRNA was synthesized *in vitro* from a TRPM3α2-encoding cDNA subcloned in a pBF1-based plasmid (kindly provided by Prof. Bernd Fakler, Freiburg, Germany) with the mMESSAGE mMACHINE SP6 kit (Ambion) according to the manufacturer's instructions. Oocytes were injected with 69 µl of TRPM3α2 cRNA (1000 ng/µl) and incubated for at least 48 h at 20° C in an oocyte medium (EcoCyte), containing (in mM): 90 NaCl, 2 KCl, 2 $CaCl_2$, 1 $MgCl_2$, 5 HEPES, 0.5 g l^{-1} polyvinylpyrrolidone, 100 U ml^{-1} penicillin, and 100 µg ml^{-1} streptomycin (pH 7.2). The pipette solution contained (in mM): 115 NaCl, 5 KCl, 1 $CaCl_2$, 10 HEPES and 50 µM PregS (pH 7.3), yielding pipette resistances of 200-500 kΩ. The bath solution contained (in mM): 130 KCl, 2 $MgCl_2$, 1 EGTA, 2 NaATP, 10 HEPES (pH 7.5). Isosakuranetin, Mg^{2+} or DMSO was added to the bath solution at the indicated concentrations. In all solutions pH was adjusted with KOH. Voltage ramps (1 mV ms^{-1}) were applied from -95.4 mV to +104.6 mV (liquid junction potential corrected by -4.6 mV) from a holding potential of -4.6 mV at a rate of 1 Hz with an EPC-10 amplifier controlled by the Patchmaster software (HEKA Instruments). Pipettes were coated

Molecular Pharmacology Fast Forward. Published on September 4, 2013 as DOI: 10.1124/mol.113.086843
This article has not been copyedited and formatted. The final version may differ from this version.

with paraffin and washed with water. Seal formation was achieved by approaching the oocyte and releasing the positive pipette pressure after cell contact. After a seal has been formed, a giant patch was excised by fast back and forth movement of the pipette. The giant patch was placed in front of a custom application system with three channels. By moving the pipette, the patch was exposed to the constantly flowing solution stream of the different application channels.

MTT viability test

To measure a possible cytotoxicity of the flavonoids, enzymatic conversion of 3-(4,5-dimethylthioazol-2-yl)-2,5-diphenyltetrazoliumbromid (MTT) was assessed. HEK293 cells were seeded onto a 96-well plate coated with poly-L-lysine (10,000 cells per well). The next day, cells were incubated with the compounds diluted in cell culture medium for at least 24 hours. For colorimetric detection, the medium was exchanged to a phenol red-free medium (100 µl per well), containing 1.2 mM MTT, and cells were placed in the incubator for 4 h. Formazan complexes that arose were solubilized with DMSO, absorbance was measured at 560 nm and at 670 nm with the transmission spectrometer head of a plate reader device (Polarstar Omega, BMG Labtech). A solvent control was set as 100% and measurements in presence of the indicated substances were normalized to this value.

Behavioral analysis

All animal experiments were conducted in accordance with the accepted standards of animal care and approved by the local authorities (regional governmental agency of the State of Saxony, Germany; TVV 02/12). 3-week old female and male C57BL/6J mice were used. For the hot plate test, isosakuranetin (2 mg kg^{-1}) and hesperetin (10 mg kg^{-1}) were dissolved in Miglyol 812 (Caesar & Loretz GmbH, Germany) containing 0.1% of DMSO, and compounds or the vehicle alone were injected intraperiotoneally (i.p; 6 ml kg^{-1}). Thirty minutes after the injection, mice were placed on a hot plate set to a temperature of 52°C. The delay to the first pain-related

Molecular Pharmacology Fast Forward. Published on September 4, 2013 as DOI: 10.1124/mol.113.086843
This article has not been copyedited and formatted. The final version may differ from this version.

response (hindpaw shaking, lifting or licking, jumping) was measured by an investigator blind to substance application. Measurements of the body temperature were performed with a digital ear infrared thermometer (Thermoscan IRT 4520, Braun, Germany) in the mice arm pit before and 30 min after injection of the compounds or vehicle.

The PregS-induced pain was assessed 30 min after i.p injection of isosakuranetin (2 mg kg^{-1}) and hesperetin (10 mg kg^{-1}) or vehicle. PregS was solved in distilled water. A volume of 10 µl containing 5 nmol of PregS was injected into the midplantar right hindpaw. The latency to, duration and number of nocifensive responses (paw licking, shaking, or lifting) were registered.

Plasma concentrations

Plasma concentrations of isosakuranetin were determined with modifications according to (Vega-Villa, et al., 2008). Male and female mice were i.p. injected with 2 or 10 mg kg^{-1} isosakuranetin, and whole blood samples were collected under anaesthesia by heart puncture. Blood samples were centrifuged to obtain the plasma, and 200 µl of plasma were mixed with 25 µl ethoxycoumarin (4 µM in acetonitrile) as internal standard and 600 µl of ice-cold acetonitrile. The plasma was stirred for 1 min and centrifuged at 12,000 g for 5 min. The supernatant was evaporated at 40°C under nitrogen and reconstituted in 100 µl 30 % acetonitrile, containing 0.2 % aqueous phosphoric acid (vol/vol) and centrifuged. Cleared supernatant (20 µl) was injected onto a HPLC column (Ultrasep ES PHARM RP18E; 5 µm, 3 mm x 150 mm) implemented in a HPLC-system with absorbance detection at 288 nm (Agilent, 1100 series; Böblingen, Germany). Separation was carried out isocratically at 30°C with a mobile phase consisting of 44 % acetonitril in 0.2 % aqueous phosphoric acid (vol/vol) with a flow of 0.55 ml min^{-1}.

Stock solutions and drugs

All modulators were dissolved in DMSO, if not indicated otherwise. The concentration of stock solutions was chosen in such a way that the DMSO concentration in the final solution never

Molecular Pharmacology Fast Forward. Published on September 4, 2013 as DOI: 10.1124/mol.113.086843
This article has not been copyedited and formatted. The final version may differ from this version.

exceeded 0.14 % at the highest test concentration of the respective modulator and further reduced by serial dilution of the compounds. PregS, pinocembrin, 4'-hydroxyflavanone, liquiritigenin, phloretin, formononetin, ononetin and hesperetin were purchased from Sigma Aldrich. Isosakuranetin was purchased from Roth.

Statistical analysis

All data are expressed as mean ± standard error of the mean (SEM). The number of cells analyzed in each experiment is indicated in the figure legends. To test for statistically significant differences, ANOVA with the Tukey´s post-hoc test was used. A probability level of $p < 0.05$ was considered as significant. The pharmacochemical properties of isosakuranetin and liquiritigenin were obtained from www.chemicalize.org.

Molecular Pharmacology Fast Forward. Published on September 4, 2013 as DOI: 10.1124/mol.113.086843
This article has not been copyedited and formatted. The final version may differ from this version.

Results

Identification of novel TRPM3-blocking flavanones

The three previously described TRPM3 blockers (Straub, et al., 2013) naringenin, hesperetin and eriodictyol differ chemically only in the substitutions on the B ring of the flavanone structure (Fig 1A). These different substitutions account for differences in the potency to block TRPM3 and for the differences in the selectivity (Straub, et al., 2013). We now tested whether flavanones with different modifications at the A or C rings are still capable of blocking TRPM3 (Fig 1). HEK293 cells stably expressing TRPM3 (HEK_{mTRPM3}) were incubated with the fluorescent calcium indicator dye Fluo-4, dispensed into 384-well plates that were prefilled with different concentrations of the flavonoids, and PregS (35 µM)-induced calcium entry was measured. Although weakly potent, 4'-hydroxyflavanone, a flavanone that has no hydroxyl group on the A ring, was still a blocker (47 % block at 25 µM) of TRPM3. Liquiritigenin, a flavanone, that has a single hydroxyl group on the A ring (C7 atom), abrogated the PregS-induced $[Ca^{2+}]_i$ signal when preincubated at a concentration of 25 µM. Pinocembrin differs from the potently TRPM3-blocking naringenin by a complete lack of hydroxyl groups on the B ring. It only partially inhibited the $[Ca^{2+}]_i$ signal, highlighting the importance of these substitutions for TRPM3 block. Conversely, isosakuranetin features a methoxy group at the C4' atom of the ring and completely blocked the PregS-induced $[Ca^{2+}]_i$ entry into HEK_{mTRPM3} cells at a concentration of 25 µM.

We were further interested if the flavanone backbone is required to block TRPM3. To this end, we investigated several compounds from different flavonoid subgroups, including the flavonol quercetin, the flavone apigenin (Fig. 1B), the flavanoles epicatechin and epigallocatechin (Fig. 1C), the isoflavones genistein, daidzein and formononetin (Fig. 1D) and the dihydrochalcone phloretin (Fig 1E). Among the tested flavonoid subgroups, only phloretin partially blocked the PregS-induced calcium entry (Fig. 1B) whereas none of the others exerted more than 20 % inhibition of PregS-induced $[Ca^{2+}]_i$ signals when applied at a concentration of 25 µM (see Fig. 1).

Molecular Pharmacology Fast Forward. Published on September 4, 2013 as DOI: 10.1124/mol.113.086843
This article has not been copyedited and formatted. The final version may differ from this version.

We conclude that the flavanone backbone and substitutions at the A and B rings are required to strongly block TRPM3. Within the tested flavanones, isosakuranetin and liquiritigenin almost completely abrogated the PregS-induced elevations of $[Ca^{2+}]_i$ in HEK_{mTRPM3} cells.

Concentration-dependence of liquiritigenin- and isosakuranetin-induced block of TRPM3-dependent Ca^{2+} entry and ionic currents

To assess the potency of the newly identified blockers, we first performed fluorometric Ca^{2+} assays in HEK_{mTRPM3} cell suspensions that were exposed to serially diluted compounds and then stimulated with 35 µM PregS. Liquiritigenin elicited a half-maximal block with an IC_{50} of 500 ± 70 nM (Fig. 2 A, B). Isosakuranetin blocked PregS-induced $[Ca^{2+}]_i$ with an IC_{50} of 50 ± 6 nM (Fig. 2 C, D). The Hill coefficients were 0.8 for liquiritigenin and 1.3 for isosakuranetin.

To characterize the impact of the more potently acting isosakuranetin on TRPM3 currents, we performed whole-cell patch clamp measurements. To reassess the concentration-response curves with the more quantitative electrophysiological method, PregS-induced currents were recorded in HEK_{mTRPM3} cells, and isosakuranetin was acutely added via the bath solution at various concentrations (Fig. 3). The isosakuranetin-induced TRPM3 block was slowly developing and recovering after removal of the modulator (Fig. 3A). Isosakuranetin blocked the inward currents at -113 mV slightly more potently (IC_{50} = 80 ± 13 nM) compared to the outward currents measured at +87 mV (IC_{50} = 120 ± 24 nM) (Fig. 3B, C). The Hill coefficients were 1.0 for both, liquiritigenin and isosakuranetin. Although the potency of TRPM3 block displayed some voltage dependence, both currents were isosakuranetin-sensitive and almost completely blocked at a concentration of 3 µM (Fig. 3D). Moreover, current-voltage relationship showed no prominent voltage-dependence of the isosakuranetin-induced TRPM3 block (Fig. 3E).

To test the biological activity of the flavanones in the heat-activated mode of TRPM3, we performed whole-cell measurements with bath solutions heated to 37-40°C. Under these conditions, inward and outward currents in TRPM3-expressing cells were partially blocked by 3

Molecular Pharmacology Fast Forward. Published on September 4, 2013 as DOI: 10.1124/mol.113.086843
This article has not been copyedited and formatted. The final version may differ from this version.

μM of isosakuranetin (Fig. 4A, B). Raising the temperature in measurements with untransfected parental HEK293 cells also yielded small inward and outward currents that remained constant in the presence of 3 μM isosakuranetin (Fig. 4C ,D). Thus, isosakuranetin presumably blocks the TRPM3-mediated component of heat-induced currents.

To assess the accessibility of the binding site and to exclude a requirement of cellular signaling cascades, we performed giant patch inside-out measurements on *Xenopus laevis* oocytes that heterologously express TRPM3 (Fig. 5). The pipette solution contained 50 μM PregS to activate TRPM3. The PregS-induced currents were strongly blocked by 1 μM or 10 μM isosakuranetin applied from the intracellular side (Fig. 5). Since high intracellular concentrations of Mg^{2+} are known to inhibit TRPM3-induced currents (Oberwinkler, et al., 2005), the inside-out configuration of the patch was confirmed by applying 10 mM Mg^{2+}. Because 10 mM Mg^{2+} are expected to eliminate TRPM3 currents, remaining inward and outward currents are likely to reflect TRPM3-unrelated leak currents that could not be subtracted because TRPM3-activating PregS in the pipette was present throughout the whole experiment. Notably, inhibition by 10 μM isosakuranetin was equally effective as the TRPM3 block by 10 mM Mg^{2+}. Since PregS binds to TRPM3 from the extracellular side (Wagner et al. 2008), whereas isosakuranetin gets access to its binding side from the intracellular side of the membrane, a competitive mechanism is unlikely. From the inside-out patch experiments we also conclude that isosakuranetin blocks TRPM3 in a membrane-confined and presumably direct fashion.

Specificity of flavanones to modulate sensory TRP channels

To evaluate the specificity of the novel TRPM3 blockers, we first examined the impact of these flavanones on the most closely related TRPM1. TRPM1 can also be activated by PregS. Unlike TRPM3, TRPM1 is strongly blocked by extracellularly applied $ZnCl_2$ (Lambert, et al., 2011). When tested at a concentration of 10 μM, liquiritigenin had almost no inhibitory effect on TRPM1-mediated $[Ca^{2+}]_i$ signals (Fig. 6A). The more potent TRPM3 blocker isosakuranetin

Molecular Pharmacology Fast Forward. Published on September 4, 2013 as DOI: 10.1124/mol.113.086843
This article has not been copyedited and formatted. The final version may differ from this version.

reduced PregS-induced $[Ca^{2+}]_i$ responses by about 36 % (Fig. 6B). In both experiments, $ZnCl_2$ (100 µM) was applied as a positive control for TRPM1 block.

TRPM3 is expressed in DRG neurons and its activation is linked to thermosensation. We therefore tested the ability of isosakuranetin and liquiritigenin to modulate other thermosensitive or sensory TRP channels, including TRPV1, TRPM8 and TRPA1. HEK293 cell lines stably expressing the respective TRP channel were loaded with Fluo-4/AM, preincubated with different concentrations of liquiritigenin or isosakuranetin, and agonist-induced increases in the Fluo-4 fluorescence were measured. Neither liquiritigenin nor isosakuranetin had an impact on the capsaicin (2 µM) induced TRPV1 activation or the menthol (300 µM) triggered activity of TRPM8 (Fig. 7A, B).

The AITC-induced TRPA1 activation was, however, concentration-dependently (2-50 µM) diminished by preincubation with either flavanone (Fig. 7A, B). Since the irritant sensor TRPA1 is activated by many chemical compounds, we performed additional $[Ca^{2+}]_i$ measurements with acutely added liquiritigenin and isosakuranetin and compared the effects to those elicited by the known TRPA1 activator AITC (30 µM). Indeed, liquiritigenin partially activated TRPA1 when acutely added at concentrations > 20 µM (Fig. 7C). Isosakuranetin also activated TRPA1 when added at concentrations > 5 µM, and activation of TRPA1 by 50 µM isosakuranetin reached levels comparable to those elicited by AITC itself (Fig. 7D).

To further evaluate the specificity of isosakuranetin and liquiritigenin among other members of the TRPM family, we investigated the blocking potency of the TRPM3-blocking compounds on endogenously expressed TRPM7 in HEK293 cells. TRPM7 is permanently blocked by divalent cations, but when patched with Mg^{2+}-free pipette solution, switching to a bath solution lacking Ca^{2+} and Mg^{2+} ions, gives rise to large inward and outward currents (Nadler, et al., 2001). Since TRPM7-like currents exhibit a fast rundown when using a Na^+-based bath solution, we used a Cs^+-based bath solution as described recently (Chubanov, et al., 2012). Neither isosakuranetin

Molecular Pharmacology Fast Forward. Published on September 4, 2013 as DOI: 10.1124/mol.113.086843
This article has not been copyedited and formatted. The final version may differ from this version.

nor liquiritigenin (20 µM each) affected TRPM7-dependent inward or outward currents in HEK293 cells (Fig. 8 A, B).

Effects of TRPM3-blocking compounds on cell viability

Since we aimed at testing biological effects of the TRPM3 blockers *in vivo*, we next assessed the cytotoxicity of the TRPM3-blocking substances in the parental HEK cell line, applying MTT tests. Within the tested compounds, liquiritigenin and ononetin did not significantly impair the cell proliferation and viability (Fig. 9). Hesperetin and isosakuranetin significantly reduced the MTT-converting enzymatic activity only partially and at the highest test concentration of 50 µM. Eriodictyol diminished the cell proliferation in concentrations of 50 µM and 25 µM, respectively. With an almost complete abrogation of the MTT conversion, naringenin was the most cytotoxic compound among the tested substances. All other flavanones were well tolerated by HEK cells at concentrations that would completely block the activation of TRPM3.

Effects of flavanones on TRPM3 in freshly isolated rat DRG neurons

To test the biological activity of novel TRPM3-blocking flavanones on endogenously expressed TRPM3, single cell calcium measurements were performed using isolated rat DRG neurons that were loaded with the Ca^{2+} indicator dye Fura-2. Functional expression of TRPM3 has previously been described in small to medium diameter neurons (Vriens, et al., 2011). Therefore, all neurons that met this criterion were selected by defining regions of interest over single cells, and all cells that were sensitive to KCl were considered as neurones. About 60-70 % of the neurons showed a PregS-induced calcium entry. A majority of, but not all PregS-positive neurons were also sensitive to stimulation with capsaicin (Fig. 10A, B). The PregS-induced calcium entry was strongly counteracted either by 5 µM isosakuranetin (Fig. 10A) or by 10 µM liquiritigenin (Fig. 10B). Since most PregS-sensitive DRG neurons also responded to stimulation with 2 µM

Molecular Pharmacology Fast Forward. Published on September 4, 2013 as DOI: 10.1124/mol.113.086843
This article has not been copyedited and formatted. The final version may differ from this version.

capsaicin or to 50 mM KCl, we conclude that TRPM3 is expressed in a subpopulation of DRG neurons that also express voltage-gated Ca^{2+} channels and very often TRPV1.

Likewise, PregS-induced currents in rat DRG neurons were partially blocked upon addition of 1 µM isosakuranetin. Similar to heterologously expressed TRPM3, the isosakuranetin-induced TRPM3 block was reversible (Fig. 10C) and showed a TRPM3 characteristic outwardly rectifying current-voltage relationship (Fig. 10D, E). PregS-induced outward currents were concentration-dependently blocked by isosakuranetin (Fig. 10F), and the potency and efficacy of the block was comparable to that seen in HEK293 cells heterologously expressing TRPM3 (see Fig. 3B).

Since isosakuranetin blocked TRPM3 in DRG neurons, we re-tested the selectivity of isosakuranetin on other sensory TRP channels within their native context. To this end, we investigated the effect of isosakuranetin (5 µM and 20 µM) on menthol- and capsaicin-induced increases in $[Ca^{2+}]_i$ in freshly isolated DRG neurons (Fig 11A-D). Isosakuranetin itself elicited a calcium entry in a small number of DRG neurons (Fig 11B, C), whereas no obvious effect was observed on menthol- and capsaicin-sensitive DRG neurons (Fig. 11D). Since overexpressed TRPA1 was partially activated by 20 µM isosakuranetin (Fig. 7D), we performed measurements in NGF-treated, TRPA1-expressing DRG neurons (Fig 11 E-H). Again, 3 of 150 and 5 of 136 DRG neurons were activated by 5 µM and 20 µM isosakuranetin, respectively. Of note, all of them also responded to the subsequent stimulation with the TRPA1 activator AITC. AITC elicited increases in $[Ca^{2+}]_i$ in 26-30% of NGF-treated DRG neurones. The previous exposure to isosakuranetin did not cause a decrease in AITC-induced $[Ca^{2+}]_i$ responses in all DRG neurons or in the AITC-sensitive subpopulation (Fig. 11H). There was also no inhibition of KCl-induced $[Ca^{2+}]_i$ signals in DRG neurons cultured either in the absence or in the presence of NGF.

Isosakuranetin and hesperetin attenuate the sensitivity of mice to noxious heat and PregS-induced pain behavior

Molecular Pharmacology Fast Forward. Published on September 4, 2013 as DOI: 10.1124/mol.113.086843
This article has not been copyedited and formatted. The final version may differ from this version.

TRPM3 has previously been shown to be involved in the perception of noxious heat *in vivo* (Vriens, et al., 2011). We therefore investigated nocifensive responses in mice that were intraperitoneally injected with TRPM3-blocking flavanones 30 minutes prior to a *hot plate* assay. Naringenin and hesperetin are citrus fruit flavanones that were often used for *in vivo* studies in mice and even in humans (Kanaze, et al., 2006). We therefore decided to perform the *in vivo* experiments with the newly identified and poorly described isosakuranetin and with hesperetin that has already been published and tested in *in vivo* studies. We preferred hesperetin over naringenin because naringenin strongly impaired cell viability of HEK293 cells in concentrations up to 12.5 µM (Fig. 9).

The latency of nocifensive behavior assessed on a hot plate (52 °C) was significantly prolonged in mice after hesperetin (10 mg kg^{-1}, i.p.) or isosakuranetin (2 or 10 mg kg^{-1}, i.p.) treatment compared to vehicle-treated animals (Fig. 12A). Note that 2 mg/kg hesperetin were not sufficient to significantly increase the pain latency.

Since antagonists of the thermosensitive TRPV1 elicited hyperthermia in different species such as rat and mouse (Gavva, et al., 2008;Gunthorpe and Chizh, 2009), we measured the temperature of mice before and 30 minutes after injection of hesperetin and isosakuranetin. As shown in Figure 12B, the newly identified TRPM3 blocker isosakuranetin or hesperetin attenuated the response to noxious heat in mice without altering their body temperature at either dosage.

The endogenous neurosteroid PregS acts as a chemical activator of TRPM3 (Wagner *et al.*, 2008) and evokes pain (Ueda, et al., 2001). Intraplantar injection of PregS (2.5, 5 and 10 nmol) dose-dependently elicited prolonged nocifensive responses, consisting of vigorous licking and lifting of the hindpaw, whereas the injection of the vehicle did not cause a nocifensive behavior (data not shown). The duration and number of nocifensive events after blocking TRPM3 by isosakuranetin and hesperetin were measured at a PregD dose of 5 nmol per injected paw. Isosakuranetin at dosages of 2 and 10 mg kg^{-1} significantly diminished the duration and the

Molecular Pharmacology Fast Forward. Published on September 4, 2013 as DOI: 10.1124/mol.113.086843
This article has not been copyedited and formatted. The final version may differ from this version.

number of nocifensive movements (Fig. 12C, D). Hesperetin injected in the same doses did not significantly reduce nocifensive responses. No differences in the latency to the first response to PregS were observed (data not shown).

Since the antinociceptive effects of both isosakuranetin doses were similar and more pronounced than those observed by applying 10 mg kg^{-1} hesperetin, indicating that isosakuranetin effects may be already saturated at a dose of 2 mg kg^{-1}. Saturating effects may be caused by its higher potency, but also by a lower percentage of conjugation. We therefore assessed the plasma concentrations that were achieved after intraperitoneal application of 10 mg kg^{-1} isosakuranetin. Peak concentrations were achieved about 10 min after the injection, but the individual variability was high (Fig. 12E). A mean plasma concentration of 5.0 ± 1.8 µg ml^{-1} (17.5 ± 6.3 µM) unconjugated isosakuranetin was measured 30 min after i.p. application and with a lower individual variability. Plasma levels then dropped rapidly, presumably due to fast formation of metabolites. 30 min after application of 2 mg ml^{-1}, the mean plasma concentration of unconjugated isosakuranetin was 1.8 µM and may be sufficient to block TRPM3.

Molecular Pharmacology Fast Forward. Published on September 4, 2013 as DOI: 10.1124/mol.113.086843
This article has not been copyedited and formatted. The final version may differ from this version.

Discussion

Owing to their low potency and to their known actions on other biological effectors, previously published TRPM3 blockers like the PPAR-γ-agonistic antidiabetic drug rosiglitazone (Majeed, et al., 2011), or the nonsteroidal antiinflammatory drug mefenamic acid (IC_{50} = 6.6 µM) (Klose, et al., 2011) have not been used to investigate TRPM3 functions *in vivo.* Starting from the recent finding that citrus fruit flavanones block TRPM3, we sought to obtain non-toxic, selective and potent TRPM3 inhibitors that may be used in animal models of pain perception. Hereby, the pharmacophore was confirmed and substituent variation led to the identification of isosakuranetin and liquiritigenin as non-cytotoxic, more potent and selective TRPM3 inhibitors. Both recombinant TRPM3 and TRPM3-related $[Ca^{2+}]_i$ signals and ionic currents in DRG neurons were strongly and reversibly inhibited. Other sensory TRP channels or TRPM1, the closest relative of TRPM3, remained largely unaffected at modulator concentrations that fully blocked TRPM3. *In vivo* application of isosakuranetin and hesperetin confirmed an antinociceptive effect on heat or PregS-induced pain responses. Interestingly, the i.p. administration of both flavanones did not affect the body temperature, an effect that would be expected for compounds with TRPV1-antagonistic properties.

Besides a hit optimization strategy, we intended to more clearly assign the pharmacophore of flavonoid that is required to block TRPM3 and to assess the impact of the hydroxylation pattern at the A and C rings. In plants, flavonoids are usually present as glycosides. Upon enteral uptake, flavonoid glycosides are metabolized in a complex fashion. After consumption of naringin, the glycoside moiety is hydrolyzed by bacteria in the distal part of the intestine (Fuhr and Kummert, 1995), and the corresponding aglycones are being absorbed. In addition to phase I modification, flavanone aglycones undergo three types of phase II conjugation reactions: methylation, sulfation and glucuronidation (Manach, et al., 2004). Accordingly, Silberberg et al. (Silberberg, et al., 2006) found plasma concentrations of 10-17 µM naringenin, but also 100-120

Molecular Pharmacology Fast Forward. Published on September 4, 2013 as DOI: 10.1124/mol.113.086843
This article has not been copyedited and formatted. The final version may differ from this version.

nM of isosakuranetin and 230 nM hesperetin after feeding rats with a diet containing 0.5% naringin. Unlike naringenin, which is extensively metabolized to its glucuronide or sulfate conjugates, 52% of isosakuranetin and 94% of hesperetin remain unconjugated and, therefore, may exert biological activities *in vivo*. Conjugated flavanone aglycones are typically eliminated with half-times in the range of about 4-8 h (Erlund, et al., 2001). To avoid possible uncertainties that may result from enteral resorption or hepatic first-pass elimination, we applied hesperetin or isosakuranetin by intraperitoneal injection.

Although the flavanone backbone appeared optimal for TRPM3 block, the hydroxylation pattern strongly impacted on the potency to block TRPM3. The C7´ hydroxylation at the A ring is favorable. The missing C5´ hydroxylation at the A ring in liquiritigenin did not improve the potency to block TRPM3 compared to naringenin, but further increased the selectivity of the effect and lowered the cytotoxicity in HEK293 cells. Concerning the B ring, hydroxylation at the C3' atom appeared unfavorable, but 4´-hydroxylation or 4´-O-methylation improved the potency to block TRPM3 without strongly compromising the blocker selectivity. Thus, adding more complex substituents at the C4´ position may provide a promising target for further investigation.

When compared to other biological activities that have been reported for flavanones, inhibition of TRPM3 by various flavanones displays a distinct and unique preference. Liquiritigenin, a flavanone found in many plants including licorice, is a selective and potent estrogen receptor β (ER-β) agonist (EC_{50} = 36.5 nM) (Mersereau, et al., 2008) and may relate to beneficial effects observed after applying a liquiritigenin-containing herbal drug (MF101) used in traditional Chinese medicine to treat menopausal symptoms (Mersereau, et al., 2008). Isoflavones from soy beans, such as genistein and daizein, also act as phytoestrogens that bind to both ERβ and ERα (Mersereau, et al., 2008;An, et al., 2001), but are poorly effective in blocking TRPM3.

Compared to our results with a higher potency of isosakuranetin to block TRPM3, the structure relationship for binding ER receptors differs from the structure needed to block TRPM3. Furthermore, glycosylation of naringenin, found in naringenin-6-C-glucoside or in naringin

Molecular Pharmacology Fast Forward. Published on September 4, 2013 as DOI: 10.1124/mol.113.086843
This article has not been copyedited and formatted. The final version may differ from this version.

enhanced the estrogenic effect (Swarnkar, et al., 2012), whereas we previously demonstrated that glycosylation in naringin and hesperedin prevents the inhibition of TRPM3 (Straub, et al., 2013).

Besides their property to bind to ER receptors, flavonoids modulated phase I metabolizing enzymes via binding to proteins of the cytochrome P450 family (CYP450). Naringenin and eriodictyol have been shown to block CYP1 activity with an IC_{50} > 4 µM. Naringenin also inhibits CYP3A4 and CYP19 (Moon, et al., 2006). With an IC_{50} of 0.34 µM, liquiritigenin has been identified as a potent inhibitor of CYP19 (Paoletta, et al., 2008). Inhibitory effects of isosakuranetin on CYP1 enzyme isoforms require concentrations in the range of 1-3 µM (Takemura, et al., 2010), and inhibition of other CYP450 enzymes has, to our knowledge, not been demonstrated. We conclude that liquiritigenin may be the TRPM3 inhibitor with the highest selectivity compared to other TRP channels. Thus, when used as a cell biological tool to profile TRP channel-related responses, liquiritigenin may be favorable. However, its effects on CYP450 enzymes and its ER-β-agonistic properties may interfere with its TRPM3-blocking properties *in vivo*. Isosakuranetin in contrary is, with respect to non-TRP channel off-target effects, a preferable compound for use in *in vivo* pharmacological studies.

The physiological and pathophysiological functions of TRPM3 are still poorly understood. Different splice variants that impede on the Ca^{2+} permeability of the pore (e.g. the α1 splicing event) (Oberwinkler, et al., 2005) or even eliminate a functional pore (Frühwald, et al., 2012) further complicate the situation. In TRPM3-deficient transgenic mice, phenotypic alterations hint to a role of TRPM3 in thermal pain perception (Vriens, et al., 2011), an effect that is closely mimicked by a pharmacological block of the channel described in the present study. Considering the expression of TRPV1 and TRPM3 in DRG neurons, the contribution of each of the heat-sensing sensory channels to thermal pain perception is intriguingly complex and seems redundant. However, pharmacological inhibition of either TRPV1 or TRPM3 exerts similar antinociceptive effects. At present, a cross-talk between both channels has not been described.

Molecular Pharmacology Fast Forward. Published on September 4, 2013 as DOI: 10.1124/mol.113.086843
This article has not been copyedited and formatted. The final version may differ from this version.

An efferent function of heat-sensitive, CGRP-releasing nociceptive neurons has been demonstrated in neurogenic inflammation, but may also contribute to the pyrexia-inducing effects of TRPV1 blockers. In contrast to TRPV1 blockers, the systemic administration of isosakuranetin did not cause a discernible increase in the body temperature. This observation hints to a promising feature of TRPM3 as a potential analgesic target molecule and may provide a strategy to avoid the adverse effects of TRPV1 blockers. The exact reason why TRPM3 block is not associated with similar side effects than inhibitors of TRPV1 is not known. Possibly, the thermal threshold of TRPM3 activation is sufficiently high to avoid regulation by physiological body or skin temperatures. Likewise, the marked shift of threshold temperatures described for TRPV1 in acidic or inflamed tissues (Gavva, et al., 2008) may not apply to TRPM3. Finally, the population of DRG neurons that express TRPV1 or TRPM3 is not completely identical (Vriens, et al., 2011). Thus, TRPM3 activation may not exactly mimic TRPV1-induced responses.

Another open question relates to possible consequences of TRPM3 inhibition other than attenuation of thermal pain sensation. Obviously, we cannot exclude that such on- or off-target effects may limit the therapeutic potential of TRPM3 inhibition. On the other hand, two lines of evidence support the assumption that TRPM3 inhibition may be tolerated: i) the phenotype of $TRPM3^{-/-}$ mice is relatively mild and ii) TRPM3-blocking compounds identified in this study are contained predominantly in citrus fruit that are part of our daily diet. In $TRPM3^{-/-}$ mice, a partially reduced pupillary response to light has been described (Hughes, et al., 2012). In contrast to a loss of TRPM1 that directly affects the function of bipolar cells in the retina, thereby causing congenital night blindness (Koike, et al., 2010) the effect of TRPM3 deficiency on pupillary responses is less pronounced (Hughes, et al., 2012). Future work will have to clarify whether acute inhibition of TRPM3 interferes with retinal functions. TRPM3 is functionally expressed in insulin-secreting beta cells. Although no obvious effects were observed in the resting blood glucose level in $TRPM3^{-/-}$ mice that exhibit no obvious developmental or metabolic deficits (Vriens, et al., 2011), the acute application of TRPM3 blockers may cause alterations of glucose

Molecular Pharmacology Fast Forward. Published on September 4, 2013 as DOI: 10.1124/mol.113.086843
This article has not been copyedited and formatted. The final version may differ from this version.

homeostasis. Using the TRPM3-blocking flavanones, these questions may be addressed and help to clarify possible endocrine functions of TRPM3 in the pancreas.

As an off-target effect of flavanones, antiinflammatory and/or antioxidant properties may add to effects on TRPM3 specifically, if pain regimes are being tested in models of inflammation. Such properties may, thus, overlap with pain-alleviating effects of the TRPM3 inhibitors e.g. in pain threshold tests with CFA-induced paw inflammation. Experimentally, the inhibition of carageenan-induced paw edema formation by orally applied (50 mg kg^{-1} day^{-1}) or intravenously injected liquiritigenin (15 mg kg^{-1} day^{-1}) has been demonstrated (Kim, et al., 2008). In a cell culture model using an LPS-primed macrophage-like cell line, Kim *et al.* observed an inhibition of cytokine production by 3-30 µM liquiritigenin. However, TRPM3 block by liquiritigenin requires lower concentrations of the flavanone. In addition, systemically administered isosakuranetin was effective to elicit antinociceptive effects at a single dose of only 2 mg kg^{-1}. Thus, the highly potent and selective TRPM3 blockers described in this study may help disentangle the on-target and off-target effects that are related to antiinflammatory or antioxidant properties of flavanones. Within this context, a pain-alleviating effect of eriodictyol, another flavanone with antioxidant properties, has been described and attributed to TRPV1 inhibition (Rossato, et al., 2011). As outlined earlier, we were unable to reproduce inhibition of TRPV1, but demonstrated that eriodictyol efficiently blocks TRPM3. Interestingly, the eriodictyol-induced antinociceptive effect was not associated with hyperthermia. Likewise, the TRPM3-blocking compounds hesperetin and isosakuranetin did not increase the body temperature. Hence, flavanones with TRP channel-inhibiting properties and/or inhibition of TRPM3 may provide a promising starting point to develop novel and tolerable analgesic therapies.

Molecular Pharmacology Fast Forward. Published on September 4, 2013 as DOI: 10.1124/mol.113.086843
This article has not been copyedited and formatted. The final version may differ from this version.

Acknowledgments

We thank Helga Sobottka, Marion Leonhardt and Raissa Wehmeyer for excellent technical assistance.

Authorship Contribution

Participated in research design: Straub, Krügel, Mohr, Rizun, Konrad, Oberwinkler, Schaefer, Teichert

Conducted experiments: Straub, Krügel, Mohr, Rizun, Konrad, Teichert

Contributed new reagents or analytic tools:

Performed data analysis: Straub, Krügel, Mohr, Rizun, Konrad, Teichert

Wrote or contributed to the writing of the manuscript: Straub, Krügel, Mohr, Rizun, Konrad, Oberwinkler, Schaefer, Teichert

Molecular Pharmacology Fast Forward. Published on September 4, 2013 as DOI: 10.1124/mol.113.086843
This article has not been copyedited and formatted. The final version may differ from this version.

References

An J, Tzagarakis-Foster C, Scharschmidt TC, Lomri N and Leitman DC (2001) Estrogen receptor β-selective transcriptional activity and recruitment of coregulators by phytoestrogens. *J Biol Chem* **276**:17808-17814.

Chubanov V, Schnitzler M, Meißner M, Schäer S, Abstiens K, Hofmann T and Gudermann T (2012) Natural and synthetic modulators of SK (Kca2) potassium channels inhibit magnesium-dependent activity of the kinase-coupled cation channel TRPM7. *Br J Pharmacol* **166**:1357-1376.

Erlund I, Meririnne E, Alfthan G and Aro A (2001) Plasma kinetics and urinary excretion of the flavanones naringenin and hesperetin in humans after ingestion of orange juice and grapefruit juice. *J Nutr* **131**:235-241.

Frühwald J, Camacho LJ, Dembla S, Mannebach S, Lis A, Drews A, Wissenbach U, Oberwinkler J and Philipp SE (2012) Alternative splicing of a protein domain indispensable for function of transient receptor potential melastatin 3 (TRPM3) ion channels. *J Biol Chem* **287**:36663-36672.

Fuhr U and Kummert AL (1995) The fate of naringin in humans: A key to grapefruit juice-drug interactions? *Clin Pharmacol Ther* **58**:365-373.

Gavva NR, Treanor JJ, Garami A, Fang L, Surapaneni S, Akrami A, Alvarez F, Bak A, Darling M, Gore A, Jang GR, Kesslak JP, Ni L, Norman MH, Palluconi G, Rose MJ, Salfi M, Tan E, Romanovsky AA, Banfield C and Davar G (2008) Pharmacological blockade of the vanilloid receptor TRPV1 elicits marked hyperthermia in humans. *Pain* **136**:202-210.

Grimm C, Kraft R, Schultz G and Harteneck C (2005) Activation of the melastatin-related cation channel TRPM3 by D-erythro-sphingosine. *Mol Pharmacol* **67**:798-805.

Gunthorpe MJ and Chizh BA (2009) Clinical development of TRPV1 antagonists: targeting a pivotal point in the pain pathway. *Drug Discov Today* **14**:56-67.

Hellwig N, Plant TD, Janson W, Schafer M, Schultz G and Schaefer M (2004) TRPV1 acts as proton channel to induce acidification in nociceptive neurons. *J Biol Chem* **279**:34553-34561.

Hoffmann A, Grimm C, Kraft R, Goldbaum O, Wrede A, Nolte C, Hanisch UK, Richter-Landsberg C, Bruck W, Kettenmann H and Harteneck C (2010) TRPM3 is expressed in sphingosine-responsive myelinating oligodendrocytes. *J Neurochem* **114**:654-665.

Hughes S, Pothecary CA, Jagannath A, Foster RG, Hankins MW and Peirson SN (2012) Profound defects in pupillary responses to light in TRPM-channel null mice: a role for TRPM channels in non-image-forming photoreception. *Eur J Neurosci* **35**:34-43.

Kanaze FI, Bounartzi MI, Georgarakis M and Niopas I (2006) Pharmacokinetics of the citrus flavanone aglycones hesperetin and naringenin after single oral administration in human subjects. *Eur J Clin Nutr* **61**:472-477.

Kim YW, Zhao RJ, Park SJ, Lee JR, Cho IJ, Yang CH, Kim SG and Kim SC (2008) Anti-inflammatory effects of liquiritigenin as a consequence of the inhibition of NF-kappaB-dependent iNOS and proinflammatory cytokines production. *Br J Pharmacol* **154**:165-173.

Molecular Pharmacology Fast Forward. Published on September 4, 2013 as DOI: 10.1124/mol.113.086843
This article has not been copyedited and formatted. The final version may differ from this version.

Klose C, Straub I, Riehle M, Ranta F, Krautwurst D, Ullrich S, Meyerhof W and Harteneck C (2011) Fenamates as TRP channel blockers: mefenamic acid selectively blocks TRPM3. *Br J Pharmacol* **162**:1757-1769.

Koike C, Numata T, Ueda H, Mori Y and Furukawa T (2010) TRPM1: a vertebrate TRP channel responsible for retinal ON bipolar function. *Cell Calcium* **48**:95-101.

Lambert S, Drews A, Rizun O, Wagner TF, Lis A, Mannebach S, Plant S, Portz M, Meissner M, Philipp SE and Oberwinkler J (2011) Transient receptor potential melastatin 1 (TRPM1) is an ion-conducting plasma membrane channel inhibited by zinc ions. *J Biol Chem* **286**:12221-12233.

Lee N, Chen J, Sun L, Wu S, Gray KR, Rich A, Huang M, Lin JH, Feder JN, Janovitz EB, Levesque PC and Blanar MA (2003) Expression and characterization of human transient receptor potential melastatin 3 (hTRPM3). *J Biol Chem* **278**:20890-20897.

Majeed Y, Bahnasi Y, Seymour VA, Wilson LA, Milligan CJ, Agarwal AK, Sukumar P, Naylor J and Beech DJ (2011) Rapid and contrasting effects of rosiglitazone on transient receptor potential TRPM3 and TRPC5 channels. *Mol Pharmacol* **79**:1023-1030.

Manach C, Scalbert A, Morand C, Rémésy C and Jiménez L (2004) Polyphenols: food sources and bioavailability. *Am J Clin Nutr* **79**:727-747.

Mersereau JE, Levy N, Staub RE, Baggett S, Zogovic T, Chow S, Ricke WA, Tagliaferri M, Cohen I, Bjeldanes LF and Leitman DC (2008) Liquiritigenin is a plant-derived highly selective estrogen receptor beta agonist. *Mol Cell Endocrinol* **283**:49-57.

Moon YJ, Wang X and Morris ME (2006) Dietary flavonoids: effects on xenobiotic and carcinogen metabolism. *Toxicol In Vitro* **20**:187-210.

Nadler MJS, Hermosura MC, Inabe K, Perraud AL, Zhu Q, Stokes AJ, Kurosaki T, Kinet JP, Penner R, Scharenberg AM and Fleig A (2001) LTRPC7 is a Mg^{2+}ATP-regulated divalent cation channel required for cell viability. *Nature* **411**:590-595.

Naylor J, Li J, Milligan CJ, Zeng F, Sukumar P, Hou B, Sedo A, Yuldasheva N, Majeed Y, Beri D, Jiang S, Seymour VA, McKeown L, Kumar B, Harteneck C, O'Regan D, Wheatcroft SB, Kearney MT, Jones C, Porter KE and Beech DJ (2010) Pregnenolone sulphate- and cholesterol-regulated TRPM3 channels coupled to vascular smooth muscle secretion and contraction. *Circ Res* **106**:1507-1515.

Noerenberg W, Sobottka H, Hempel C, Ploetz T, Fischer W, Schmalzing G and Schaefer M (2012) Positive allosteric modulation by ivermectin of human but not murine P2X7 receptors. *Br J Pharmacol* **167**:48-66.

Nörenberg W, Hempel C, Urban N, Sobottka H, Illes P and Schaefer M (2011) Clemastine potentiates the human P2X7 receptor by sensitizing it to lower ATP concentrations. *J Biol Chem* **286**:11067-11081.

Oberwinkler J, Lis A, Giehl KM, Flockerzi V and Philipp SE (2005) Alternative splicing switches the divalent cation selectivity of TRPM3 channels. *J Biol Chem* **280**:22540-22548.

Paoletta S, Steventon GB, Wildeboer D, Ehrman TM, Hylands PJ and Barlow DJ (2008) Screening of herbal constituents for aromatase inhibitory activity. *Bioorg Med Chem* **16**:8466-8470.

Molecular Pharmacology Fast Forward. Published on September 4, 2013 as DOI: 10.1124/mol.113.086843
This article has not been copyedited and formatted. The final version may differ from this version.

Rossato MF, Trevisan G, Walker CI, Klafke JZ, de Oliveira AP, Villarinho JG, Zanon RB, Royes LF, Athayde ML, Gomez MV and Ferreira J (2011) Eriodictyol: a flavonoid antagonist of the TRPV1 receptor with antioxidant activity. *Biochem Pharmacol* **81**:544-551.

Silberberg M, Gil-Izquierdo A, Combaret L, Remesy C, Scalbert A and Morand C (2006) Flavanone metabolism in healthy and tumor-bearing rats. *Biomed Pharmacother* **60**:529-535.

Straub I, Mohr F, Stab J, Konrad M, Philipp S, Oberwinkler J and Schaefer M (2013) Citrus fruit and fabacea secondary metabolites potently and selectively block TRPM3. *Br J Pharmacol* **168**:1835-1850.

Swarnkar G, Sharan K, Siddiqui JA, Mishra JS, Khan K, Khan MP, Gupta V, Rawat P, Maurya R, Dwivedi AK, Sanyal S and Chattopadhyay N (2012) A naturally occurring naringenin derivative exerts potent bone anabolic effects by mimicking oestrogen action on osteoblasts. *Br J Pharmacol* **165**:1526-1542.

Takemura H, Itoh T, Yamamoto K, Sakakibara H and Shimoi K (2010) Selective inhibition of methoxyflavonoids on human CYP1B1 activity. *Bioorg Med Chem* **18**:6310-6315.

Ueda H, Inoue M, Yoshida A, Mizuno K, Yamamoto H, Maruo J, Matsuno K and Mita S (2001) Metabotropic neurosteroid/sigma-receptor involved in stimulation of nociceptor endings of mice. *J Pharmacol Exp Ther* **298**:703-710.

Urban N, Hill K, Wang L, Kuebler WM and Schaefer M (2012) Novel pharmacological TRPC inhibitors block hypoxia-induced vasoconstriction. *Cell Calcium* **51**:194-206.

Vega-Villa KR, Remsberg CM, Podelnyk KL and Davies NM (2008) Stereospecific high-performance liquid chromatographic assay of isosakuranetin in rat urine. *J Chromatogr B Analyt Technol Biomed Life Sci* **875**:142-147.

Vriens J, Owsianik G, Hofmann T, Philipp SE, Stab J, Chen X, Benoit M, Xue F, Janssens A, Kerselaers S, Oberwinkler J, Vennekens R, Gudermann T, Nilius B and Voets T (2011) TRPM3 is a nociceptor channel involved in the detection of noxious heat. *Neuron* **70**:482-494.

Wagner TF, Loch S, Lambert S, Straub I, Mannebach S, Mathar I, Dufer M, Lis A, Flockerzi V, Philipp SE and Oberwinkler J (2008) Transient receptor potential M3 channels are ionotropic steroid receptors in pancreatic beta cells. *Nat Cell Biol* **10**:1421-1430.

Molecular Pharmacology Fast Forward. Published on September 4, 2013 as DOI: 10.1124/mol.113.086843
This article has not been copyedited and formatted. The final version may differ from this version.

Footnotes

This work was supported by the Deutsche Forschungsgemeinschaft (DFG) within the framework of FOR 806 (to M.S), and the SFB 593 (to J.O).

Molecular Pharmacology Fast Forward. Published on September 4, 2013 as DOI: 10.1124/mol.113.086843
This article has not been copyedited and formatted. The final version may differ from this version.

Legends for Figures

Figure 1: Chemical structures of flavonoids and their potency to block TRPM3. Flavonoids can be divided into different subgroups: **A**) flavanones, (**B**) flavones (apigenin) and flavonols (quercetin), (**C**) flavanols, (**D**) isoflavanones and (**E**) dihydrochalkones. To clarify the blocking-potency of the different flavonoid subgroups, HEK_{mTRPM3} cells were incubated with the calcium indicator dye Fluo-4. Cells were dispensed into 384-well plates that were prefilled with single flavonoids (25 µM), and fluorescence intensities were measured during PregS-induced activation of TRPM3.

Figure 2: Identification of isosakuranetin and liquiritigenin as novel potent inhibitor of TRPM3. Fluo4-loaded HEK293 cells stably expressing TRPM3 were incubated with different concentrations of isosakuranetin and liquiritigenin and fluorescence intensities were measured during injection of the TRPM3 activator pregnenolone sulphate (PregS). (**A**) Examples of calcium entry traces extracted from a single 384-well plate measurement, each trace represents a different liquiritigenin concentration. Light grey trace shows a solvent control. (**B**) Concentration-response curve of liquiritigenin. TRPM3 activation without an inhibitor (DMSO control) was set as 100% and fluorescence intensities evoked by solutions containing inhibitors were normalized to this value. (**C**), (**D**) Similar experiments as described for isosakuranetin. (**C**) Example traces of a single 384-well measurement with different concentrations of isosakuranetin. (**D**) Concentration-response curve of isosakuranetin. Data represent at least 4 independent experiments for liquiritigenin and 5 independent experiments for isosakuranetin with duplicates each. Shown are means and S.E.M. IC_{50} values and Hill coefficients (n) were obtained by non-linear curve fitting, applying a four parameter Hill equation.

Molecular Pharmacology Fast Forward. Published on September 4, 2013 as DOI: 10.1124/mol.113.086843
This article has not been copyedited and formatted. The final version may differ from this version.

Figure 3: Electrophysiologically measured concentration-response curves of isosakuranetin-induced TRPM3 block. Whole-cell recordings of HEK_{mTRPM3} cells stimulated with 20 µM of PregS and blocked with different concentrations of isosakuranetin were performed to obtain concentration-response curves. Due to the channel rundown, an interpolated value between before and after isosakuranetin-induced block was used to calculate the percentage of block. (**A**)**,** (**B**) Representative recordings of whole-cell currents obtained from voltage steps from -113 mV (lower trace, open circles) to 87 mV (upper trace, black circles). Dotted line: zero current level. (**C**) Concentration-response curves of isosakuranetin to block PregS-induced inward currents (open circles; -113 mV) and outward currents (black circles; +87 mV). IC_{50} values and Hill coefficients (n) were obtained by non-linear curve fitting, applying a four parameter Hill equation. Each data point represents means ± S.E.M of 5 - 12 independent experiments. (**D**) Representative whole-cell currents from a HEK_{mTRPM3} cell activated with 35 µM of PregS and blocked with 3 µM of isosakuranetin. Data are extracted from voltage ramps and depict the current at 87 mV (upper trace) and –113 mV (lower trace). Arrows show the respective data point that was used to obtain I/V curves shown in (**E**). (**E**) Current-voltage relationship of PregS-induced TRPM3 currents before (1) and after block with 3 µM of isosakuranetin (2). (Iso = isosakuranetin)

Figure 4: Isosakuranetin blocks heat-induced TRPM3 currents in transiently transfected HEK293 cells. (**A**) Representative whole-cell recording from a HEK293 cell transiently transfected with a TRPM3-encoding plasmid. During the recording, the superfused bath solution was heated to 37-40°C, and outward (+87 mV) and inward currents (-113 mV) were recorded. 40 s after the onset of heating, 3 µM isosakuranetin (Iso) was added to the bath solution. Dotted line: zero current level. (**B**) Statistical analysis of peak current densities in 6 independent measurements performed as shown in (**A**). (**C**) Representative whole-cell currents in a non-

Molecular Pharmacology Fast Forward. Published on September 4, 2013 as DOI: 10.1124/mol.113.086843
This article has not been copyedited and formatted. The final version may differ from this version.

transfected HEK293 cell recorded as described in (**A**). (**D**) Statistical analysis of peak current densities of 4 independent measurements as shown in (**C**).

Figure 5: Isosakuranetin applied to the cytosolic side of oocyte giant patches blocks PregS-induced TRPM3 currents. (**A**) Example recording of an inside-out giant patch excised from a *Xenopus leavis* oocyte expressing TRPM3. PregS (50 µM), applied via the pipette to the extracellular side of the patch, activated TRPM3 currents that were reversibly blocked with 10 µM isosakuranetin (Iso) or with 10 mM Mg^{2+}. Data are extracted from voltage ramps and depict the current at +80 mV (upper trace) and –80 mV (lower trace). Arrows indicate the time points of I/V curves shown in (**B**). (**B**) I/V curve of PregS-activated TRPM3 currents before (1) and during superfusion with 10 µM isosakuranetin (2) or with 10 mM Mg^{2+} (3). (**C**) Similar experiment as in (**A**), but with 1 µM isosakuranetin (**D**) I/V curve of PregS-activated TRPM3 currents measured in (**C**) before (1) and during superfusion with 1 µM isosakuranetin (2) or 10 mM Mg^{2+} (3). (**E,F**) Statistical analysis of currents at +80 mV (**E**) and -80 mV (**F**) recorded in PregS-stimulated giant patches treated with solvent (0.02 % DMSO), 1 µM or 10 µM isosakuranetin, or with 10 mM Mg^{2+}. Data were obtained from 5-10 independent measurements each.

Figure 6: Effects of liquiritigenin and isosakuranetin on Ca^{2+} entry through TRPM1. Single cell calcium imaging experiments were performed with HEK293 cells transiently transfected with cDNA plasmids encoding TRPM1 and loaded with the fluorometric Ca^{2+} indicator Fura-2/AM. TRPM1 was activated with 50 µM PregS alone and in the presence of 10 µM isosakuranetin (Iso; n = 55) (**A**) or 10 µM liquiritigenin (Liqu; n = 48) (**B**), followed by application of PregS alone and in combination with 100 µM $ZnCl_2$. Shown are means and SEM of at least 4-6 independent imaging experiments.

Molecular Pharmacology Fast Forward. Published on September 4, 2013 as DOI: 10.1124/mol.113.086843
This article has not been copyedited and formatted. The final version may differ from this version.

Figure 7: Effects of liquiritigenin and isosakuranetin on other sensory TRP channels. HEK293 Fluo-4 loaded cells stably expressing the indicated TRP channels were dispensed into 384-well plates and preincubated with either liquiritigenin (**A**) or isosakuranetin (**B**). Activation of the respective channel was followed by measuring increases in the fluorescence intensity, or in $HEK_{rTRPV1:CFP}$ cells, by monitoring the Ca^{2+} influx-mediated intracellular acidification, causing a decrease in the fluorescence intensity of co-expressed YFP (Hellwig, et al., 2004). The respective activators are 2 µM capsaicin for TRPV1, 30 µM AITC for TRPA1 and 300 µM menthol for TRPM8. Acute stimulation of HEK293 cells stably expressing TRPA1 with liquiritigenin (**C**) and isosakuranetin (**D**) led to an activation of TRPA1. Data represents means and S.E.M of 4-6 different experiments, performed in duplicate each.

Figure 8: Endogenously expressed TRPM7 in HEK293 cells is not affected by isosakuranetin or liquiritigenin. (**A**) Representative whole cell recordings from HEK293 cells endogenously expressing TRPM7. Perfusion of the cells with a solution containing no divalent cations elicited linear TRPM7-like currents. An additional perfusion with 20 µM isosakuranetin or 20 µM liquiritigenin did not significantly influence the TRPM7 current. (**B**) Descriptive statistics of 5-10 independent measurements performed as shown in (A).

Figure 9: Effect of TRPM3-blocking flavanones on cell viability. HEK293 cells were incubated with different concentrations of TRPM3-blocking flavanones and cell viability was detected by performing a MTT viability test. Data represent mean values and S.E.M. of at least 5-8 independent experiments. To test for statistical significant differences, ANOVA with Tukey´s post-hoc test was performed with the normalized data (* $p < 0.05$; ** $p < 0.01$).

Figure 10: PregS-evoked Ca^{2+} influx in rat DRG neurons is reduced by liquiritigenin or isosakuranetin. (**A**), (**B**) Freshly dissociated DRG neurons were loaded with Fura-2/AM, and

Molecular Pharmacology Fast Forward. Published on September 4, 2013 as DOI: 10.1124/mol.113.086843
This article has not been copyedited and formatted. The final version may differ from this version.

the $[Ca^{2+}]_i$ was measured in individual neurons. Cells were superfused with 50 µM PregS and (**A**) simultaneously with 5 µM of isosakuranetin, or 10 µM liquiritigenin (**B**), followed by stimulation with 2 µM capsaicin and addition of 50 mM KCl to select neuronal cells that express voltage-gated Ca^{2+} channels. (**C**) Example trace of whole-cell currents from a freshly isolated rat DRG neuron measured in a Na^+-free extracellular solution. Data are extracted from voltage ramps and depict the current at +100 mV (upper trace) and –100 mV (lower trace). The neuron was perfused with 50 µM PregS alone or in combination with 1 µM isosakuranetin. (**D**) Current-voltage relationship before stimulation (1), after stimulation with PregS (2), and after addition of 1 µm isosakuranetin (3). (**E**) Current-voltage relationship of the PregS-induced current depicted as the difference between trace 2 and 1 in panel (**D**). (**F**) Example of a whole cell measurement of a DRG neuron as described in (**D**) during perfusion with PregS and various concentrations of isosakuranetin. Shown are currents at +100 mV (dotted line: zero current level).

Figure 11: Isosakuranetin does not inhibit TRPM8, TRPV1 or TRPA1 channels in rat DRG neurons. Single cell calcium imaging experiments were performed with freshly isolated DRG neurons. (**A-C**) DRG neurons were superfused with solutions containing no isosakuranetin (**A**) or with solutions containing 5 µM (**B**) and 20 µM (**C**) isosakuranetin. DRG neurons were sequentially challenged with 300 µM menthol, 1 µM capsaicin and 50 mM KCl. $[Ca^{2+}]_i$ traces of cells that responded to isosakuranetin, menthol and capsaicin were grouped and highlighted by green, blue and red colors, respectively. Numbers of responsive cells are given in the application bars. (**D**) Statistical analysis of $[Ca^{2+}]_i$ determined in DRG neurons treated with buffer (open bars), with 5 µM isosakuranetin (hatched bars), or with 20 µM isosakuranetin (filled bars). Colored bars reflect results determined only in menthol-positive (blue) or in capsaicin-responding (red) subpopulations. (**E-G**) Experiments were performed essentially as in (**A-C**), but in NGF-treated DRG neurones that were stimulated with 20 µM AITC (yellow lines). (**H**) Statistical analysis of all DRG neurons measured in (**E-G**) and in the AITC-positive subpopulation (yellow

Molecular Pharmacology Fast Forward. Published on September 4, 2013 as DOI: 10.1124/mol.113.086843
This article has not been copyedited and formatted. The final version may differ from this version.

bars). Data represent 4 (**A-C**) or 3 (**E-G**) independent experiments for each condition performed with DRG neurons from different animals.

Figure 12: Isosakuranetin and hesperetin diminish the sensitivity of mice to noxious heat and attenuate the PregS-induced pain behavior. (**A**) Mice were intraperitoneally (I.p.) injected with solvent (control), with 2 mg kg^{-1} and 10 mg kg^{-1} isosakuranetin (Iso), or with 2 mg kg^{-1} and 10 mg kg^{-1} hesperetin (Hes), and placed onto a hot plate (52°C) 30 min after the injection. The latency to the first nocifensive response was recorded. (**B**) Body temperature was measured prior to (grey bars) and 30-35 min after (black bars) injection of hesperetin or isosakuranetin, respectively. (**C, D**) Chemical pain was evoked 30 min after i.p. application of the flavanones (performed as described in **A**) by intraplantar injection of PregS (5 nmol in 10 µl) into the right hindpaw. The duration (**C**) and number (**D**) of nocifensive behavioral events (paw licking, shaking, or lifting) was recorded and counted. Data represent means ± SEM of 9-12 mice per group, * $p < 0.05$. (**E**) Blood was obtained from mice sacrificed without receiving isosakuranetin (0 min) or at the indicated time points after injection of 10 mg kg^{-1} isosakuranetin (i.p.). Concentrations of unconjugated isosakuranetin were determined by HPLC and ultraviolet light spectroscopy.

A

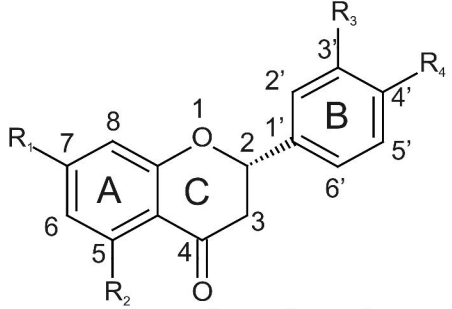

	R_1	R_2	R_3	R_4	% inhibition [25 µM]
naringenin	-OH	-OH	-H	-OH	100
eriodictyol	-OH	-OH	-OH	-OH	100
hesperetin	-OH	-OH	-OH	$-O-CH_3$	100
pinocembrin	-OH	-OH	-H	-H	17.5
liquiritigenin	-OH	-H	-H	-OH	100
4'-hydroxyflavanone	-H	-H	-H	-OH	47.3
isosakuranetin	-OH	-OH	-H	$-O-CH_3$	100

B

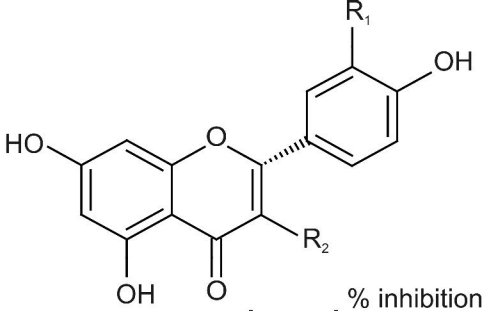

	R_1	R_2	% inhibition [25 µM]
quercetin	-OH	-OH	11.7
apigenin	-H	-H	0

C

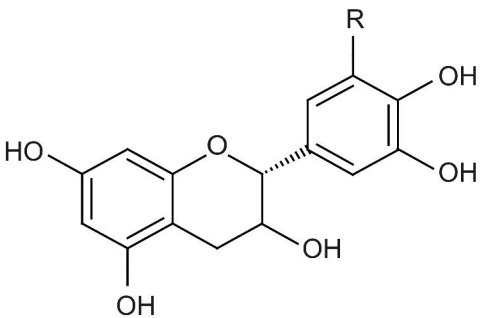

	R	% inhibition [25 µM]
epicatechin	-H	0
epigallocatechin	-OH	0

D

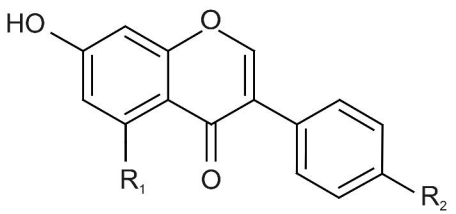

	R_1	R_2	% inhibition [25 µM]
genistein	-OH	-OH	4.1
daidzein	-H	-H	17.5
formononetin	-H	$-O-CH_3$	17.9

E

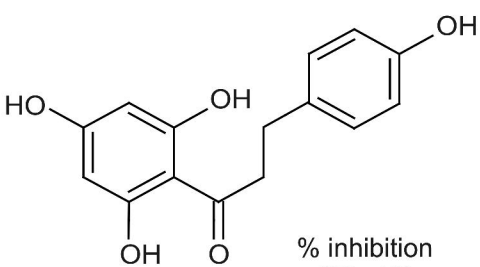

	% inhibition [25 µM]
phloretin	60.3

Figure 1

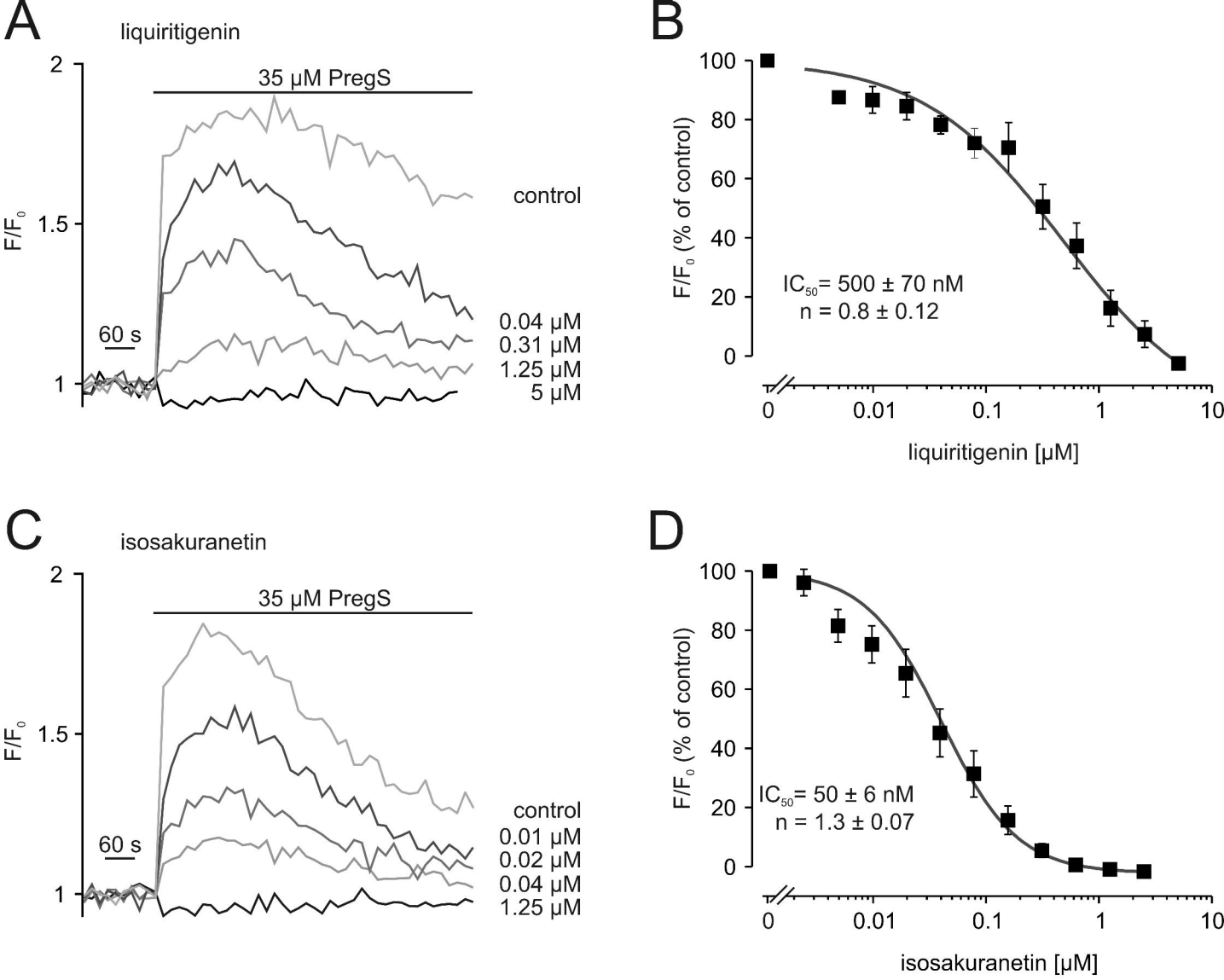
A
liquiritigenin
35 μM PregS
F/F0
2
1.5
1
60 s
control
0.04 μM
0.31 μM
1.25 μM
5 μM
B
F/F0 (% of control)
100
80
60
40
20
0
IC50= 500 ± 70 nM
n = 0.8 ± 0.12
0
0.01
0.1
1
10
liquiritigenin [μM]
C
isosakuranetin
35 μM PregS
F/F0
2
1.5
1
60 s
control
0.01 μM
0.02 μM
0.04 μM
1.25 μM
D
F/F0 (% of control)
100
80
60
40
20
0
IC50= 50 ± 6 nM
n = 1.3 ± 0.07
0
0.01
0.1
1
10
isosakuranetin [μM]

Figure 2

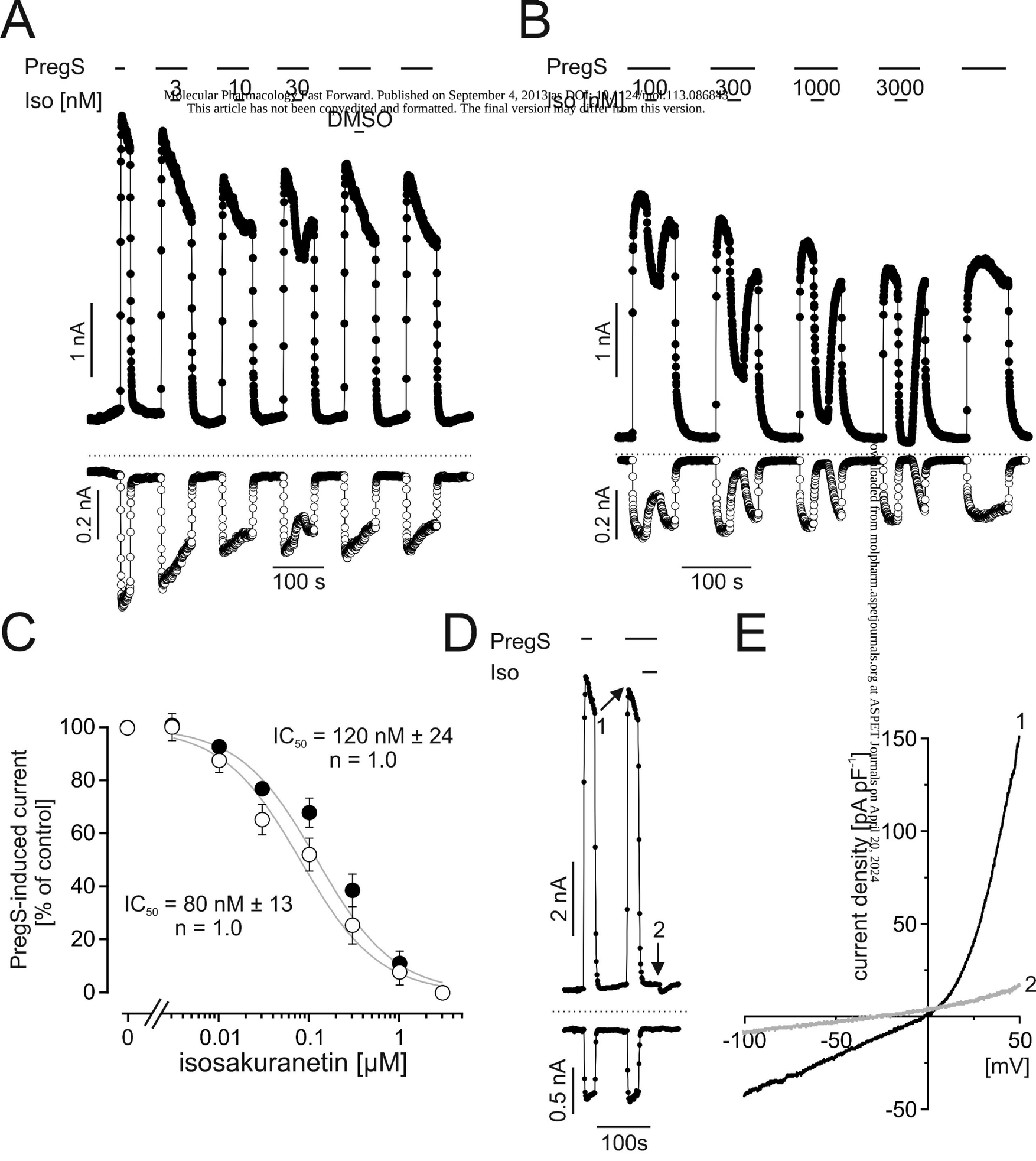

Figure 3

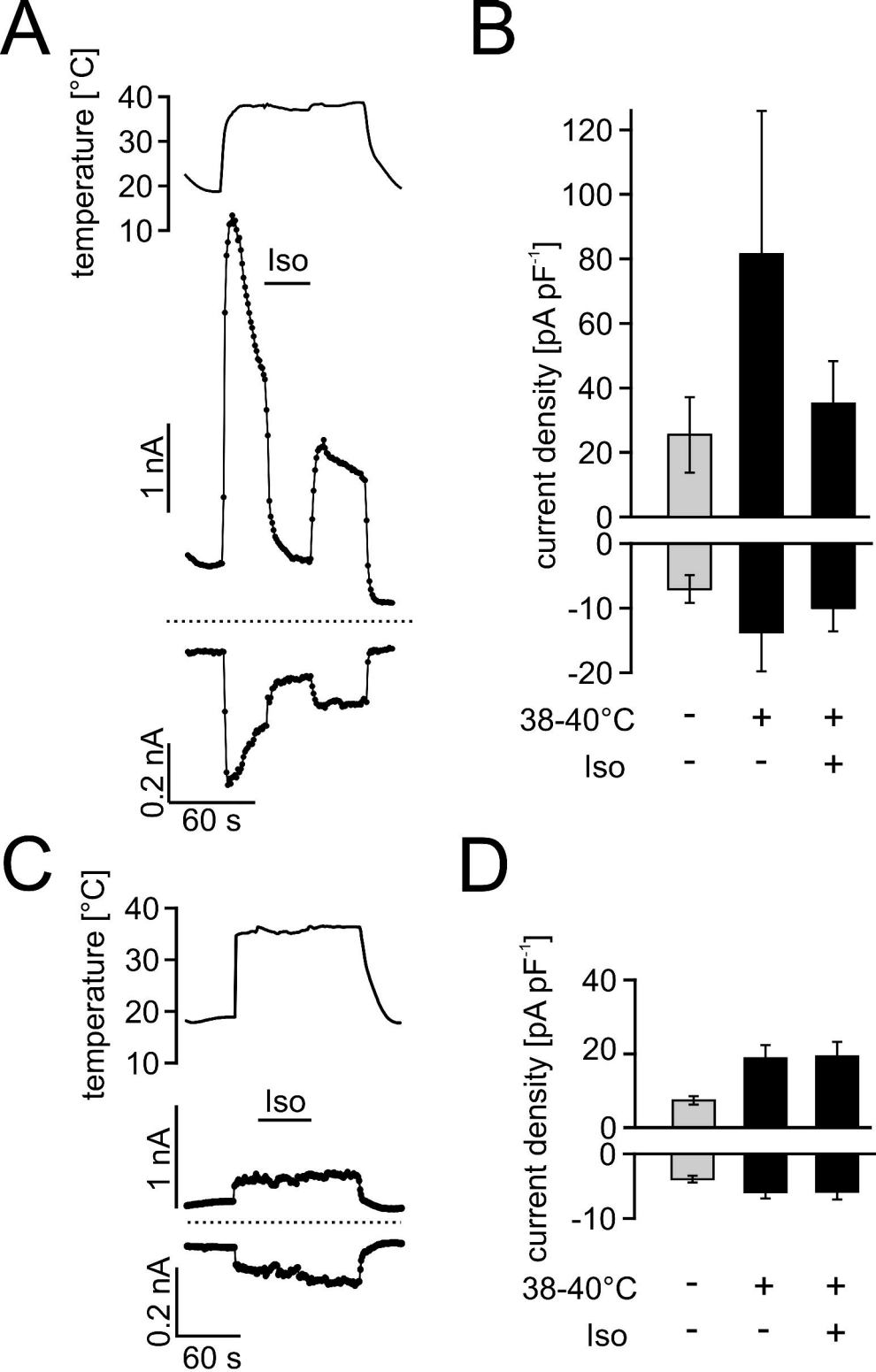
A
temperature [°C]
40
30
20
10
Iso
1 nA
0.2 nA
60 s
B
current density [pA pF⁻¹]
120
100
80
60
40
20
0
0
-10
-20
38-40°C - + +
Iso - - +
C
temperature [°C]
40
30
20
10
Iso
1 nA
0.2 nA
60 s
D
current density [pA pF⁻¹]
40
20
0
0
-10
38-40°C - + +
Iso - - +

Figure 4

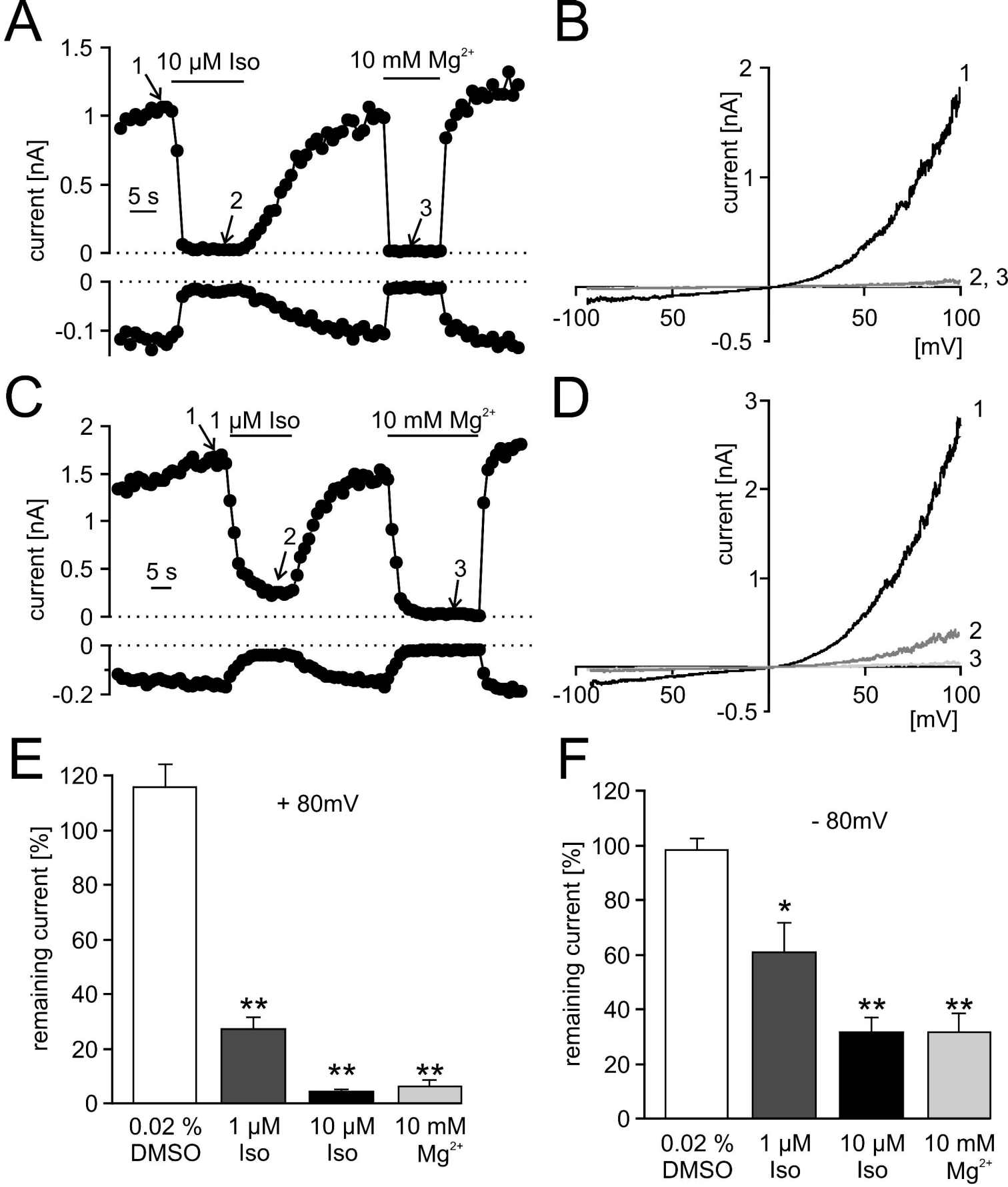
A
1.5
1
0.5
0
current [nA]
1
10 µM Iso
10 mM Mg2+
5 s
2
3
0
-0.1
B
2
1
current [nA]
1
2, 3
-100
50
50
100
-0.5
[mV]
C
2
1.5
1
0.5
0
current [nA]
1
1 µM Iso
10 mM Mg2+
2
5 s
3
0
-0.2
D
3
2
1
current [nA]
1
2
3
-100
50
50
100
-0.5
[mV]
E
120
100
80
60
40
20
0
remaining current [%]
+ 80mV
**
**
**
0.02 % DMSO
1 µM Iso
10 µM Iso
10 mM Mg2+
F
120
100
80
60
40
20
0
remaining current [%]
- 80mV
*
**
**
0.02 % DMSO
1 µM Iso
10 µM Iso
10 mM Mg2+

Figure 5

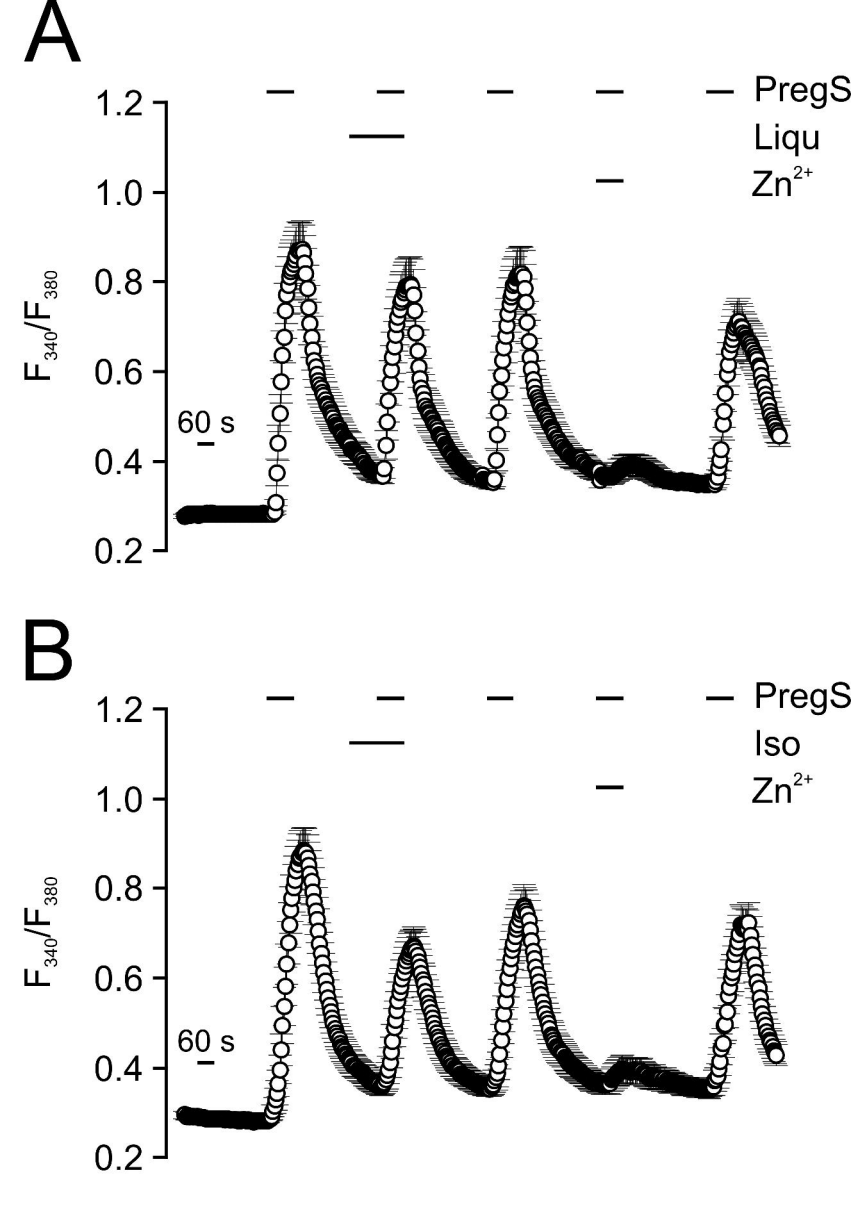
A
PregS
Liqu
Zn2+
F340/F380
1.2
1.0
0.8
0.6
0.4
0.2
60 s
B
PregS
Iso
Zn2+
F340/F380
1.2
1.0
0.8
0.6
0.4
0.2
60 s

Figure 6

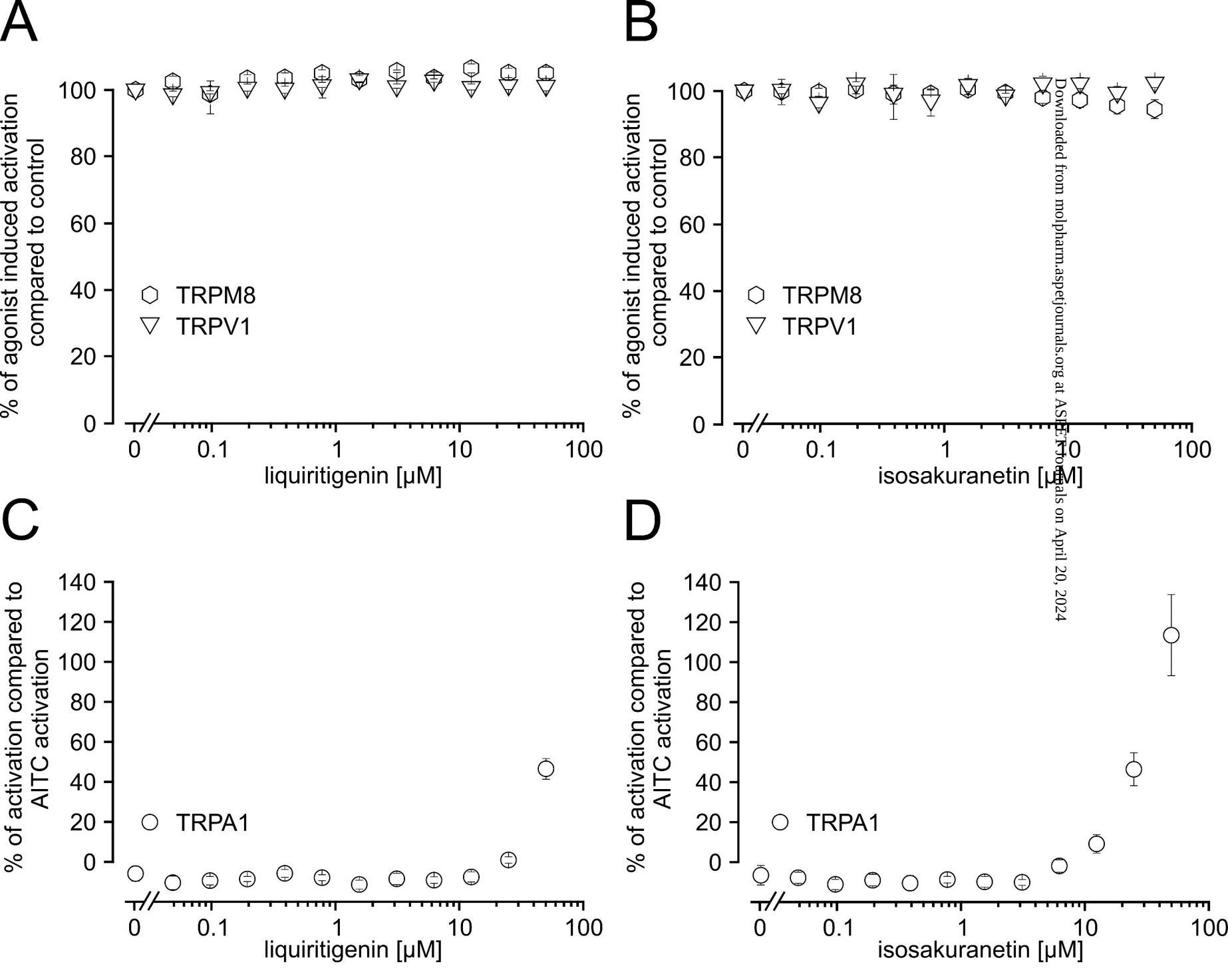

Figure 7

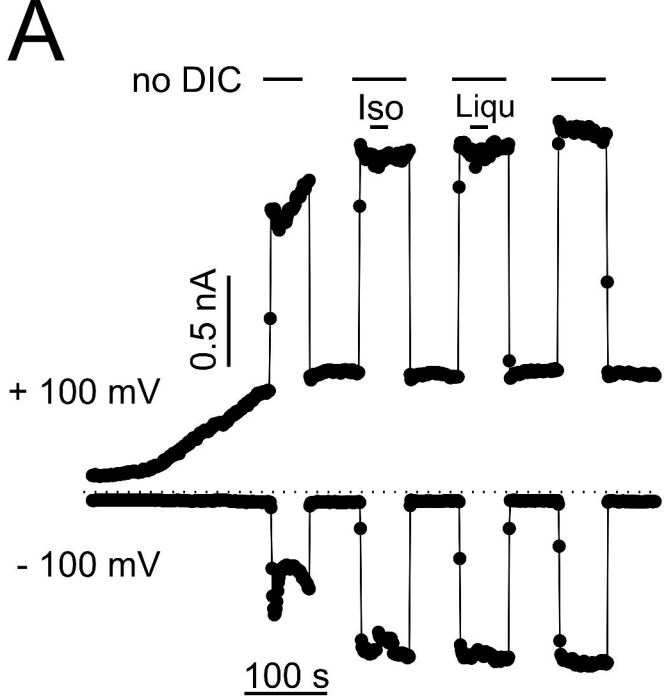
A
no DIC
Iso
Liqu
0.5 nA
+ 100 mV
- 100 mV
100 s

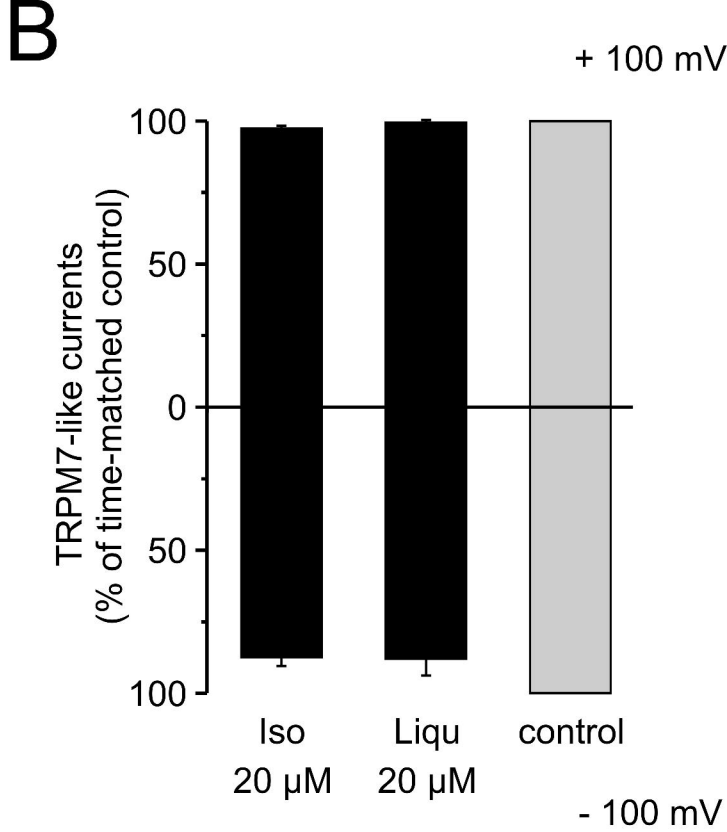
B
+ 100 mV
100
50
0
50
100
TRPM7-like currents
(% of time-matched control)
Iso
20 µM
Liqu
20 µM
control
- 100 mV

Figure 8

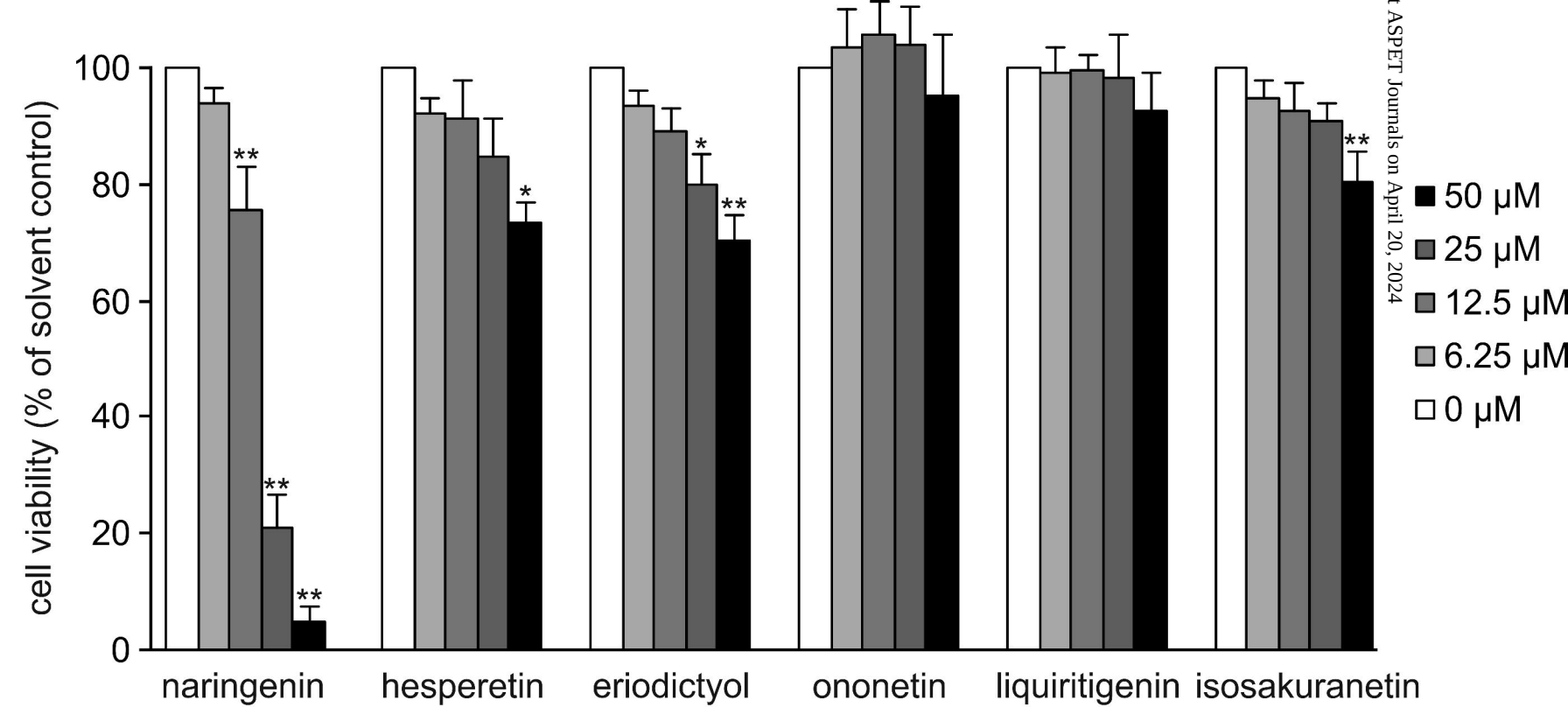

Figure 9

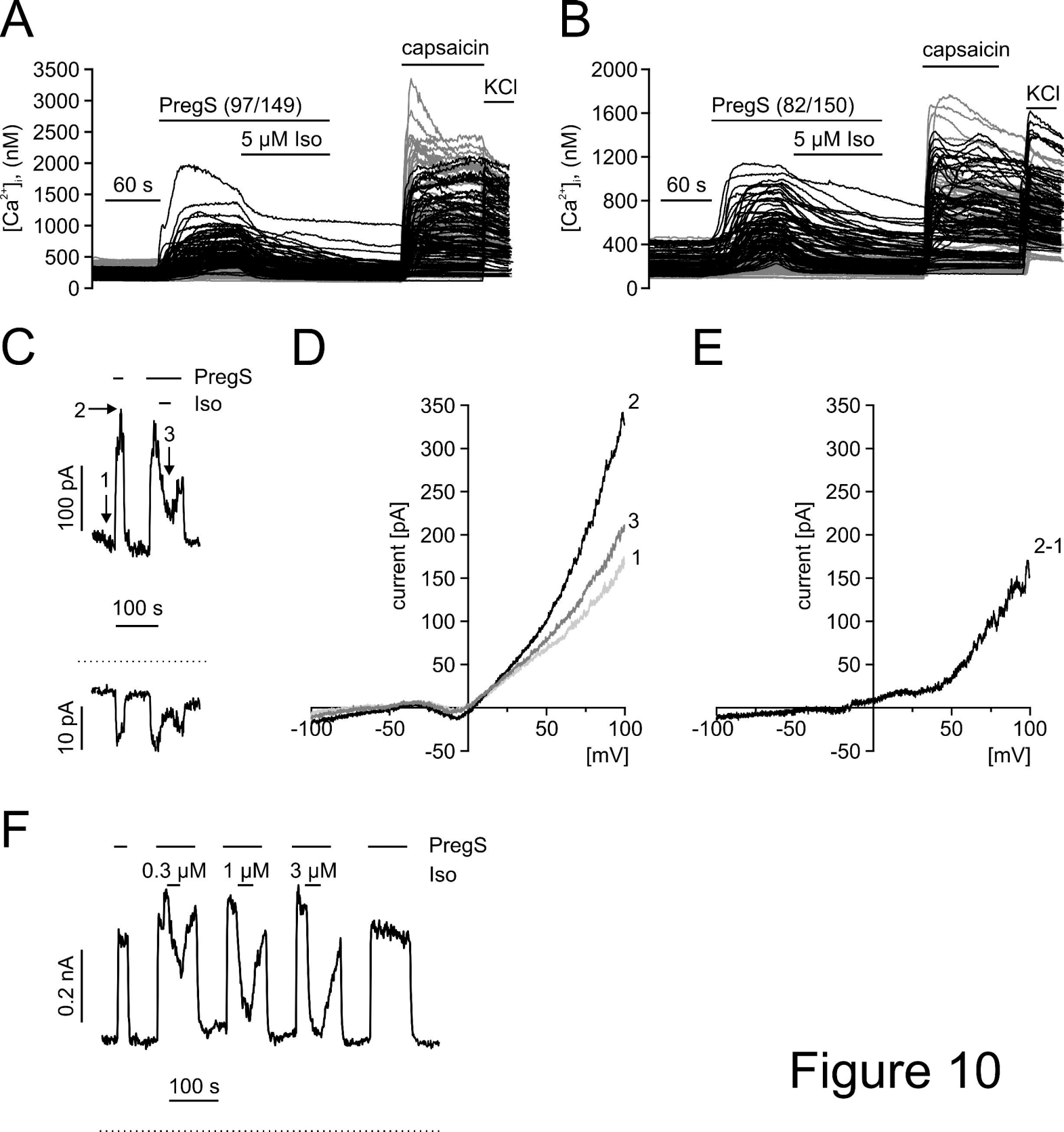
A
capsaicin
KCl
PregS (97/149)
5 μM Iso
60 s
[Ca2+]i, (nM)
3500
3000
2500
2000
1500
1000
500
0
B
capsaicin
KCl
PregS (82/150)
5 μM Iso
60 s
[Ca2+]i, (nM)
2000
1600
1200
800
400
0
C
PregS
Iso
2
3
1
100 pA
100 s
10 pA
D
current [pA]
350
300
250
200
150
100
50
-50
-100
-50
50
100
[mV]
2
3
1
E
current [pA]
350
300
250
200
150
100
50
-50
-100
-50
50
100
[mV]
2-1
F
PregS
Iso
0.3 μM
1 μM
3 μM
0.2 nA
100 s

Figure 10

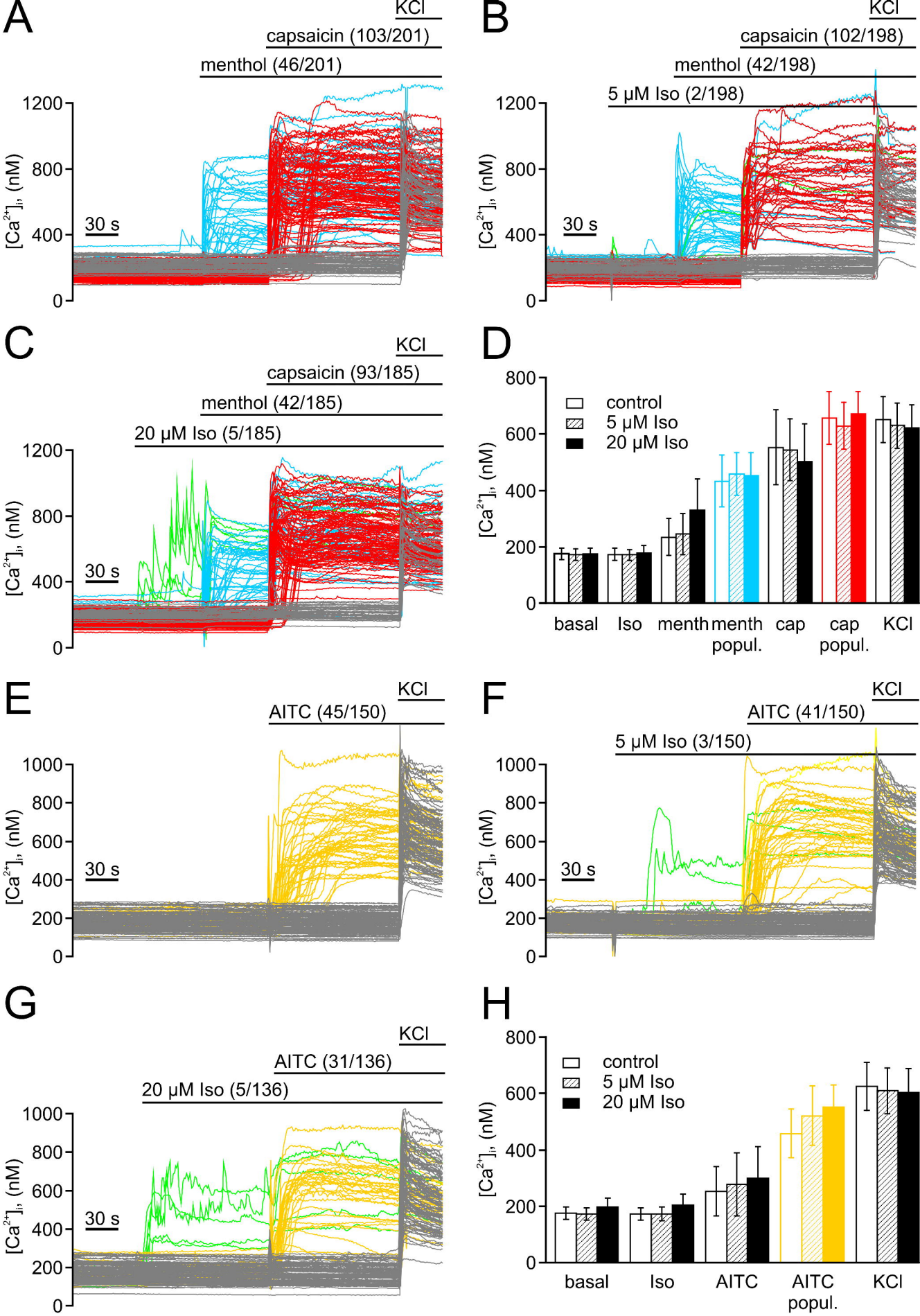
A
KCl
capsaicin (103/201)
menthol (46/201)
1200
800
400
0
[Ca2+]i (nM)
30 s
B
KCl
capsaicin (102/198)
menthol (42/198)
5 μM Iso (2/198)
1200
800
400
0
[Ca2+]i (nM)
30 s
C
KCl
capsaicin (93/185)
menthol (42/185)
20 μM Iso (5/185)
1200
800
400
0
[Ca2+]i (nM)
30 s
D
800
600
400
200
0
[Ca2+]i (nM)
control
5 μM Iso
20 μM Iso
basal
Iso
menth
menth popul.
cap
cap popul.
KCl
E
KCl
AITC (45/150)
1000
800
600
400
200
0
[Ca2+]i (nM)
30 s
F
KCl
AITC (41/150)
5 μM Iso (3/150)
1000
800
600
400
200
0
[Ca2+]i (nM)
30 s
G
KCl
AITC (31/136)
20 μM Iso (5/136)
1000
800
600
400
200
0
[Ca2+]i (nM)
30 s
H
800
600
400
200
0
[Ca2+]i (nM)
control
5 μM Iso
20 μM Iso
basal
Iso
AITC
AITC popul.
KCl

Figure 11

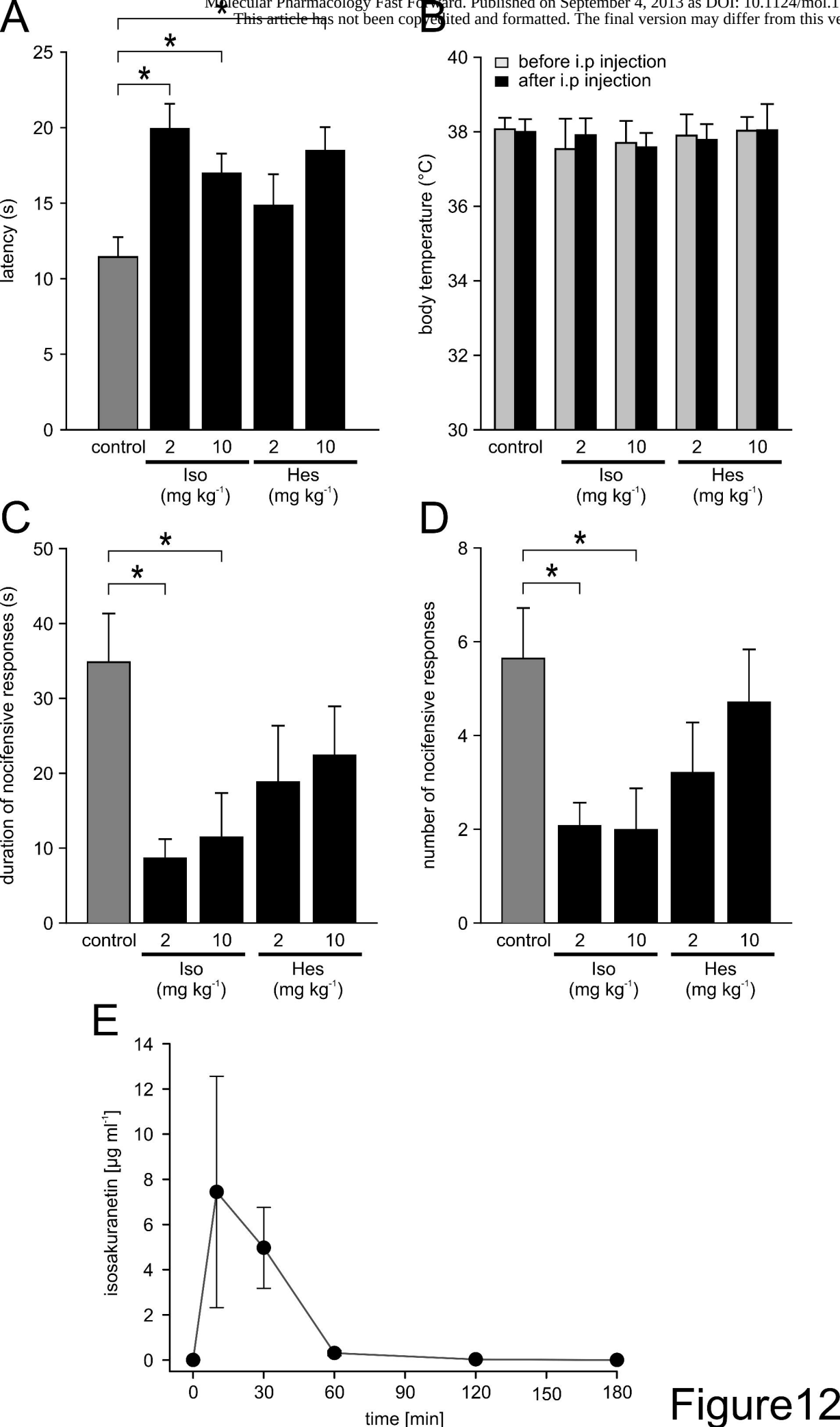

Figure12